



A hybrid phylogenetic–phylogenomic approach for species tree estimation in African *Agama* lizards with applications to biogeography, character evolution, and diversification



Adam D. Leaché^{a,*}, Philipp Wagner^{b,c}, Charles W. Linkem^a, Wolfgang Böhme^b, Theodore J. Papenfuss^d, Rebecca A. Chong^e, Brian R. Lavin^f, Aaron M. Bauer^c, Stuart V. Nielsen^g, Eli Greenbaum^h, Mark-Oliver Rödelⁱ, Andreas Schmitz^j, Matthew LeBreton^k, Ivan Ineich^k, Laurent Chirio^k, Caleb Ofori-Boateng^l, Edem A. Eniang^m, Sherif Baha El Dinⁿ, Alan R. Lemmon^o, Frank T. Burbrink^p

^a Department of Biology & Burke Museum of Natural History and Culture, University of Washington, Seattle, WA 98195-1800, USA

^b Zoologisches Forschungsmuseum Alexander Koenig, Adenauerallee 160, D53113 Bonn, Germany

^c Department of Biology, Villanova University, 800 Lancaster Avenue, Villanova, PA 19085, USA

^d Museum of Vertebrate Zoology, University of California, Berkeley, CA 94720, USA

^e Department of Biology, Colorado State University, Fort Collins, CO 80523-1878, USA

^f Department of Biology, Sonoma State University, Rohnert Park, CA 94928, USA

^g Department of Biology, Box 1848, University of Mississippi, University, MS 38677, USA

^h Department of Biological Sciences, University of Texas at El Paso, 500 West University Ave., El Paso, TX 79968, USA

ⁱ Museum für Naturkunde, Leibniz Institute for Research on Evolution and Biodiversity, 10115 Berlin, Germany

^j Department of Herpetology and Ichthyology, Natural History Museum of Geneva, C.P. 6434, CH-1211, Geneva 6, Switzerland

^k Muséum National d'Histoire Naturelle, Département Systématique et Evolution (Reptiles), ISYEB (Institut Systématique, Evolution, Biodiversité, UMR 7205 CNRS/EPHE/MNHN), Paris, France

^l Forestry Research Institute of Ghana, P.O. Box 63, Fumesua, Kumasi, Ghana

^m Department of Forestry and Wildlife, University of Uyo, Akwa Ibom State, Nigeria

ⁿ Nature Conservation Sector, Egyptian Environmental Affairs Agency, 3 Abdalla El Katib, Apt. 3, Dokki, Cairo, Egypt

^o Department of Scientific Computing, Florida State University, Dirac Science Library, Tallahassee, FL 32306-4102, USA

^p Department of Biology, The College of Staten Island, The City University of New York, Staten Island, NY 10314, USA

ARTICLE INFO

Article history:

Received 18 February 2014

Revised 24 May 2014

Accepted 14 June 2014

Available online 25 June 2014

Keywords:

Africa

Agamidae

Anchored phylogenomics

Next-generation sequencing

Sequence capture

Xenagama

ABSTRACT

Africa is renowned for its biodiversity and endemism, yet little is known about the factors shaping them across the continent. African *Agama* lizards (45 species) have a pan-continental distribution, making them an ideal model for investigating biogeography. Many species have evolved conspicuous sexually dimorphic traits, including extravagant breeding coloration in adult males, large adult male body sizes, and variability in social systems among colorful versus drab species. We present a comprehensive time-calibrated species tree for *Agama*, and their close relatives, using a hybrid phylogenetic–phylogenomic approach that combines traditional Sanger sequence data from five loci for 57 species (146 samples) with anchored phylogenomic data from 215 nuclear genes for 23 species. The Sanger data are analyzed using coalescent-based species tree inference using BEAST, and the resulting posterior distribution of species trees is attenuated using the phylogenomic tree as a backbone constraint. The result is a time-calibrated species tree for *Agama* that includes 95% of all species, multiple samples for most species, strong support for the major clades, and strong support for most of the initial divergence events. Diversification within *Agama* began approximately 23 million years ago (Ma), and separate radiations in Southern, East, West, and Northern Africa have been diversifying for >10 Myr. A suite of traits (morphological, coloration, and sociality) are tightly correlated and show a strong signal of high morphological disparity within clades, whereby the subsequent evolution of convergent phenotypes has accompanied diversification into new biogeographic areas.

© 2014 Elsevier Inc. All rights reserved.

* Corresponding author.

E-mail address: leache@uw.edu (A.D. Leaché).

1. Introduction

African *Agama* lizards are among the most diverse and widespread terrestrial squamates in Africa, making them an ideal group for investigating biogeography and conducting comparative ecological and evolutionary studies (Leaché et al., 2009; Geniez et al., 2011; Gonçalves et al., 2012; Mediannikov et al., 2012). Some *Agama* exhibit extreme sexual dimorphism, and extravagant adult male breeding coloration is among the most conspicuous traits in the genus (Wagner et al., 2011). Species with brilliantly colored males are also usually larger in size compared to females, but adult male body sizes in *Agama* can vary widely in maximum snout–vent length (SVL) from small *A. gracilimembris* (47 mm) in West Africa and the Sahel to large *A. caudospinosa* (133 mm) in East Africa. Social systems are also variable within *Agama*, with some species forming colonies composed of a single male with many females, whereas males of some species are solitary. This suite of traits is assumed to be the result of sexual selection, and in this study we quantify the correlations among these characters, and investigate the evolution of these traits in relation to phylogeny, biogeography and diversification.

Comparative genomics data are becoming increasingly easy to obtain for molecular phylogenetic studies of non-model organisms (reviewed by Lemmon and Lemmon, 2013; McCormack et al., 2013). Sequence capture approaches (also referred to as hybrid enrichment) are emerging as a popular option for obtaining phylogenomic data, because they can provide data capable of resolving difficult phylogenetic problems at deep (Crawford et al., 2012) and shallow levels (Smith et al., 2014). Sequence capture methods use short probes (60–120 base pairs) to hybridize to specific genomic regions that are then isolated and sequenced using next-generation sequencing (Gnirke et al., 2009). Competing techniques for sequence capture exploit different aspects of the genome for probe hybridization, including ultraconserved elements (Faircloth et al., 2012), conserved regions (Lemmon et al., 2012), or protein-coding genes (Li et al., 2013). Regardless of which genomic regions are exploited for hybridization, the approach offers genome-wide sampling of large numbers of loci.

A current challenge in molecular phylogenetics is the integration of phylogenomic data with traditional multilocus data (“Sanger” data). The dimensions of the data matrices are typically transposed in terms of numbers of samples and numbers of loci, with the phylogenomic data containing hundreds of loci for relatively few samples, whereas Sanger data generally contain relatively few loci with dense taxonomic sampling. Combining these different types of data introduces extensive levels of missing data, and this precludes the application of coalescent-based species tree inference methods that require independent loci to be sampled for each species. Even if data were present for all species at every locus, large numbers of loci impose computational limitations that prevent the application of most species tree inference methods.

In this study, we estimate the phylogenetic relationships among African *Agama* species using traditional multilocus data obtained using Sanger sequencing and with phylogenomic data obtained using sequence capture (Lemmon et al., 2012). The Sanger data contain 146 specimens (representing 57 species) and five independent loci (four nuclear genes and mitochondrial DNA), whereas the phylogenomic data include 23 species and 215 loci. We use a hybrid phylogenetic–phylogenomic approach to obtain a species tree for *Agama* that benefits from the properties of both types of data. The Sanger data offer the dense taxonomic sampling necessary for a comprehensive species-level phylogeny, and the phylogenomic data provide dense locus sampling for strengthening the backbone of the phylogenetic tree.

2. Materials and methods

2.1. Sanger data

2.1.1. Molecular methods

Our taxonomic sampling within *Agama* includes 95% of the described valid taxa (43 of 45 taxa, including described species and subspecies) and multiple samples for most species (116 specimens total; average = 2.7 samples/species). Outgroups include six genera belonging to the African/West Asian Agamidae clade (*Acanthocercus*, *Laudakia* [recently recognized as *Stellagama*], *Phrynocephalus*, *Pseudotrapelus*, *Trapelus*, and *Xenagama*), and *Calotes versicolor* from the South Asian sister clade (Macey et al., 2000, 2006) is used to root phylogenetic trees when necessary. A total of 146 specimens representing 57 species are included in the phylogenetic analyses (Table 1).

We collected traditional multilocus data using Sanger sequencing to obtain nearly complete taxonomic coverage with multiple samples within species. The Sanger data includes five loci: mitochondrial DNA (mtDNA) and four single copy protein coding nuclear genes. The mtDNA data (1207 aligned base pairs) includes fragments of the 16S rRNA gene (16S), the ND4 protein-coding gene (ND4), and the adjacent histidine, serine, and leucine tRNA genes (*tRNAs*). The nuclear genes (2793 aligned base pairs) include neurotrophin-3 (*NT3*), oocyte maturation factor Mos (*CMOS*), pinin gene (*PNN*), and RNA fingerprint protein 35 (*R35*). Molecular lab protocols for Sanger sequencing follow Leaché et al. (2009), and primer sequences are provided in Table 2.

2.1.2. Alignment and partitioning

Multiple sequence alignments were estimated for the indel-rich 16S and *tRNAs* using SATé v2.0.3 (Liu et al., 2011). SATé uses maximum likelihood (ML) to estimate phylogenetic trees and multiple sequence alignments simultaneously using a divide-and-conquer realignment technique, which can boost alignment accuracy substantially (Liu et al., 2009). Initial alignments were generated using ClustalW v2.0.12 (Thompson et al., 1994), and subsequent alignment refinement steps in SATé used MUSCLE v3.8 (Edgar, 2004a, 2004b) in conjunction with ML trees estimated with RAxML v7.2.6 (Stamatakis, 2006) under the GTRGAMMA model. SATé was run for 12 h with default parameter values.

The molecular genetic data were partitioned into 17 distinct data blocks including 15 blocks for the 1st, 2nd, and 3rd codon positions for each of the five protein-coding genes (e.g., *ND4*, *CMOS*, *PNN*, *NT3*, and *R35*) and two blocks for the non-coding 16S gene and *tRNAs* (treated as one block). Nucleotide substitution models for each data block were selected using jModelTest v0.1.1 (Posada, 2008). Three substitution model types were evaluated on a fixed BIONJ-JC tree, and model selection was conducted using the Bayesian information criteria (BIC). We used PartitionFinder v0.9 (Lanfear et al., 2012) to identify the optimal partitioning scheme for the 17 data blocks, and the best-fit nucleotide substitution model for each partition. We ran PartitionFinder twice with the models of molecular evolution restricted to those that are available in either MrBayes v3.2.1 (Ronquist et al., 2012) or RAxML. All PartitionFinder analyses used the greedy search algorithm, linked branch lengths in calculations of likelihood scores, and the BIC for selecting among alternative partitioning strategies.

2.1.3. Gene tree estimation

Gene trees were inferred using maximum likelihood and Bayesian inference. Gene trees were estimated from the Sanger data for each nuclear locus separately, the combined mtDNA data, the combined nuclear data, and the concatenated mtDNA and nuclear data. Analyses of protein-coding genes used codon partitioning.

Table 1

Voucher specimen information and Genbank accession numbers for Sanger sequences. The complete Sanger and anchored phylogenomics data are available on Dryad. Anchored phylogenomics data were collected for the 23 specimens highlighted in bold.

Species	Voucher	16S	ND4	CMOS	NT3	R35	PNN
<i>Acanthocercus annectans</i>	CAS 227508	JX668128	JX857621	JX838886	JX839175	JX839078	JX838995
<i>Acanthocercus annectans</i>	MVZ 242740	JX668129	JX857561	JX838887	JX839176	JX839079	JX838996
<i>Acanthocercus atricollis</i>	CAS 201727	JX668130	JX857596	JX838888	JX839177	JX839080	JX838997
<i>Acanthocercus atricollis</i>	EBG 1761	JX668131	JX857574	JX838889	JX839178	–	JX838998
<i>Acanthocercus atricollis</i>	EBG 2167	JX668132	JX857631	JX838890	JX839179	JX839081	–
<i>Acanthocercus atricollis</i>	MVZ 265804	JX668133	JX857555	JX838891	–	JX839082	JX838999
<i>Acanthocercus atricollis</i>	ZFMK 61662	JX668134	JX857632	–	–	–	–
<i>Acanthocercus cyanogaster</i>	MVZ 257904	JX668135	JX857609	JX838892	–	–	JX839000
<i>Acanthocercus cyanogaster</i>	MVZ 257924	JX668136	JX857562	JX838893	–	–	–
<i>Acanthocercus cyanogaster</i>	MVZ 257928	JX668137	JX857548	JX838894	JX839180	JX839083	JX839001
<i>Acanthocercus cyanogaster</i>	MVZ 257937	JX668138	JX857628	JX838895	–	JX839084	–
<i>Acanthocercus cyanogaster</i>	MVZ 257938	JX668139	JX857602	JX838896	–	JX839085	–
<i>Acanthocercus yemenensis</i>	MVZ 236454	JX668140	JX857608	JX838897	JX839181	JX839086	JX839002
<i>Acanthocercus yemenensis</i>	MVZ 236455	JX668141	JX857559	JX838898	JX839182	JX839087	–
<i>Agama aculeata</i>	AMNH 141775	JX668142	JX857573	JX838899	JX839183	JX839088	JX839003
<i>Agama aculeata</i>	MCZ 237841	JX668143	JX857566	JX838900	JX839184	JX839089	JX839004
<i>Agama aculeata</i>	MVZ 198076	GU128430	GU128467	JX838901	JX839185	JX839090	JX839005
<i>Agama africana</i>	ULM 200	GU128440	GU128477	JX838902	JX839186	JX839091	JX839006
<i>Agama agama</i>	MCZ 184560	JX668144	JX857595	JX838903	JX839187	JX839092	JX839007
<i>Agama agama</i>	ZFMK 15222	GU133323	–	–	–	–	–
<i>Agama anchietae</i>	AMB 4906	JX668145	JX857610	JX838904	JX839188	JX839093	JX839008
<i>Agama anchietae</i>	AMB 7582	GU128446	GU128483	JX838905	JX839189	JX839094	JX839009
<i>Agama anchietae</i>	MCZ 237865	JX668146	JX857592	JX838906	JX839190	–	–
<i>Agama anchietae</i>	ZFMK 72906	JX668147	–	JX838907	JX839191	JX839095	JX839010
<i>Agama armata</i>	AMB 8317	JX668148	JX857615	JX838908	JX839192	JX839096	JX839011
<i>Agama armata</i>	AMB 8350	JX668149	JX857598	–	JX839193	JX839097	JX839012
<i>Agama armata</i>	CAS 198929	JX668150	JX857620	JX838909	JX839194	JX839098	JX839013
<i>Agama armata</i>	CHI 201	JX668151	JX857580	JX838910	JX839195	JX839099	–
<i>Agama armata</i>	ZFMK 84990	GU128447	GU128484	–	–	JX839100	–
<i>Agama atra</i>	AMB 4487	JX668152	JX857616	JX838911	JX839196	JX839101	JX839014
<i>Agama atra</i>	AMB 4826	JX668153	JX857567	JX838912	JX839197	–	–
<i>Agama atra</i>	ZFMK 41744	JX668154	JX857569	JX838913	JX839198	JX839102	–
<i>Agama boensis</i>	KU 291845	JX668155	JX857589	JX838914	–	JX839103	JX839015
<i>Agama boensis</i>	TR 496	JX668156	JX857575	JX838915	–	JX839104	JX839016
<i>Agama bottegi</i>	CAS 227496	JX668157	JX857587	JX838916	JX839199	JX839105	–
<i>Agama boueti</i>	6251X	JX668158	–	JX838917	JX839200	JX839106	–
<i>Agama boueti</i>	6253X	JX668159	JX857557	JX838918	JX839201	JX839107	JX839017
<i>Agama boueti</i>	FMNH 262261	JX668160	JX857623	JX838919	JX839202	JX839108	JX839018
<i>Agama boueti</i>	MNCN 43869	JN665051	–	–	–	–	–
<i>Agama boueti</i>	MNHN IV	JX668161	JX857551	JX838920	JX839203	JX839109	JX839019
<i>Agama boueti</i>	MVZ 238892	JX668162	JX857613	JX838921	JX839204	JX839110	JX839020
<i>Agama boueti</i>	ZFMK 80057	GU133313	–	–	–	–	–
<i>Agama boulengeri</i>	MNHN I	GU133324	JX857619	JX838989	JX839205	JX839169	JX839021
<i>Agama boulengeri</i>	MVZ 235763	JX668163	JX857603	JX838923	JX839206	JX839112	JX839022
<i>Agama boulengeri</i>	MVZ 235764	GU128449	GU128486	JX838924	–	–	–
<i>Agama boulengeri</i>	ZFMK 76868	JX668164	–	–	–	JX839113	–
<i>Agama castroviejoi</i>	MNCN 41779	AY522929	–	–	–	–	–
<i>Agama castroviejoi</i>	MVZ 235766	GU128454	GU128491	JX838925	–	JX839114	JX839023
<i>Agama caudospinosa</i>	ZFMK 83662	GU128450	GU128487	JX838926	–	JX839115	JX839024
<i>Agama cf. benueensis</i>	FR 2235X	JX668165	JX857588	–	–	–	–
<i>Agama cf. benueensis</i>	FR 2826X	JX668166	JX857601	–	–	–	–
<i>Agama cf. benueensis</i>	FR 4218X	GU128451	GU128488	–	–	–	–
<i>Agama cristata</i>	TR 3449	JF520717	–	–	–	–	–
<i>Agama cristata</i>	TR 3450	JF520718	–	–	–	–	–
<i>Agama dodomae</i>	ZFMK 84983	JX668167	JX857552	JX838927	–	JX839116	JX839025
<i>Agama doriae</i>	MVZ 257967	JX668168	JX857614	JX838928	JX839207	–	–
<i>Agama doriae</i>	MVZ 257968	JX668169	JX857629	JX838929	–	JX839117	–
<i>Agama doriae</i>	MVZ 257970	JX668170	JX857600	JX838930	–	–	–
<i>Agama doriae</i>	MVZ 257971	JX668171	JX857622	JX838931	–	–	JX839026
<i>Agama etoshae</i>	ZFMK 21966	JX668172	JX857544	JX838932	–	–	JX839027
<i>Agama finchi</i>	ZFMK 83653	GU128452	GU128489	JX838933	–	JX839118	JX839028
<i>Agama gracilimembris</i>	UWBM 5576	JX668173	JX857617	JX838934	–	JX839119	JX839029
<i>Agama gracilimembris</i>	UWBM 5577	JX668174	JX857563	JX838935	–	JX839120	JX839030
<i>Agama gracilimembris</i>	UWBM 5578	JX668175	JX857611	JX838936	–	JX839121	JX839031
<i>Agama hartmanni</i>	ZFMK 27598	JX668176	JX857590	–	–	–	–
<i>Agama hispida</i>	AMB 4800	GU128453	GU128490	JX838937	JX839208	JX839122	JX839032
<i>Agama hispida</i>	AMB 5625	JX668177	JX857594	JX838938	JX839209	JX839123	JX839033
<i>Agama impalearis</i>	2934I	JX668178	JX857625	JX838939	JX839210	JX839124	JX839034
<i>Agama impalearis</i>	AJ414684	AJ414684	–	–	–	–	–
<i>Agama insularis</i>	KU 291843	JX668179	JX857593	–	–	JX839125	–
<i>Agama insularis</i>	TR 500	JX668180	JX857583	JX838940	JX839211	JX839126	JX839035
<i>Agama insularis</i>	TR 554	JX668181	JX857550	JX838941	JX839212	JX839127	JX839036
<i>Agama insularis</i>	TR 555	GU133325	–	JX838942	JX839213	JX839128	JX839037
<i>Agama insularis</i>	ZFMK 88247	JX668182	JX857633	JX838943	–	–	–

(continued on next page)

Table 1 (continued)

Species	Voucher	16S	ND4	CMOS	NT3	R35	PNN
<i>Agama kaimosae</i>	ZFMK 82075	JX668183	JX857630	–	–	–	–
<i>Agama kirkii</i>	MVZ 265806	JX668184	JX857624	JX838944	–	JX839129	JX839038
<i>Agama kirkii</i>	MVZ 265812	JX668185	JX857549	JX838945	–	JX839130	JX839039
<i>Agama kirkii</i>	MVZ 265827	–	JX857570	JX838946	–	JX839131	JX839040
<i>Agama kirkii</i>	MVZ 265828	JX668186	JX857558	JX838947	–	–	JX839041
<i>Agama kirkii</i>	ZFMK 54533	JX668187	–	–	–	–	–
<i>Agama knobeli</i>	AMB 4305	JX668188	JX857546	JX838948	JX839214	JX839132	JX839042
<i>Agama knobeli</i>	AMB 4670	JX668189	JX857547	JX838949	JX839215	JX839133	–
<i>Agama knobeli</i>	AMB 4850	JX668190	JX857556	JX838950	JX839216	JX839134	JX839043
<i>Agama knobeli</i>	CAS 193435	GU128448	GU128485	JX838951	JX839217	JX839135	–
<i>Agama knobeli</i>	MCZ A38433	JX668191	JX857577	JX838952	JX839218	JX839136	JX839044
<i>Agama lebretoni</i>	CAS 207957	JX668192	JX857627	JX838953	JX839219	JX839137	JX839045
<i>Agama lebretoni</i>	MVZ 253099	GU128444	GU128481	JX838954	JX839220	JX839138	JX839046
<i>Agama lionotus</i>	CAS 199008	JX668193	JX857597	JX838955	–	–	–
<i>Agama lionotus</i>	NMK L/2720	JX668194	–	–	–	–	–
<i>Agama lionotus</i>	ZFMK 82064	JX668195	–	–	–	–	–
<i>Agama lionotus</i>	ZFMK 83646	GU128456	GU128493	JX838956	JX839221	JX839139	JX839047
<i>Agama makarikarica</i>	ZFMK 18369	JX668196	–	JX838957	JX839222	JX839140	JX839048
<i>Agama makarikarica</i>	ZFMK 18370	JX668197	–	JX838958	–	JX839141	JX839049
<i>Agama montana</i>	CAS 168911	JX668198	JX857579	JX838959	JX839223	JX839142	JX839050
<i>Agama montana</i>	FMNH 251324	JX668199	JX857582	JX838960	JX839224	JX839143	JX839051
<i>Agama mossambica</i>	ZFMK 13479	JX668200	–	–	–	–	–
<i>Agama mwanzae</i>	ZFMK 82076	GU128457	–	JX838961	–	–	–
<i>Agama parafricana</i>	MVZ 249605	JX668201	JX857612	JX838962	JX839225	JX839144	JX839052
<i>Agama paragama</i>	ZFMK 15244	GU133321	–	–	–	–	–
<i>Agama picticauda</i>	29011	JX668202	JX857626	JX838963	JX839226	JX839145	JX839053
<i>Agama picticauda</i>	AMNH 109799	GU128441	GU128478	JX838964	JX839227	JX839146	JX839054
<i>Agama picticauda</i>	MVZ 238891	GU128443	GU128480	JX838965	JX839228	JX839147	JX839055
<i>Agama picticauda</i>	NCSM 76789	JX668203	–	JX838966	JX839229	JX839148	–
<i>Agama picticauda</i>	ZFMK 73845	JX668204	JX857605	JX838967	–	JX839149	–
<i>Agama picticauda</i>	ZFMK 76838	GU128442	GU128479	JX838968	JX839230	JX839150	JX839056
<i>Agama picticauda</i>	ZMB 71577	JX668205	JX857543	JX838969	JX839231	–	JX839057
<i>Agama planiceps</i>	AMB 7638	GU128458	GU128494	JX838970	JX839232	JX839151	JX839058
<i>Agama planiceps</i>	MCZ A38908	JX668206	JX857571	JX838971	JX839233	JX839152	JX839059
<i>Agama robecchii</i>	ZFMK 37812	JX668207	JX857607	–	–	JX839153	–
<i>Agama rueppelli</i>	MVZ 241336	JX668208	JX857599	JX838972	JX839234	JX839154	JX839060
<i>Agama rueppelli</i>	MVZ 241337	JX668209	JX857604	JX838973	JX839235	–	–
<i>Agama rueppelli</i>	MVZ 241338	JX668210	JX857581	JX838974	JX839236	–	–
<i>Agama rueppelli</i>	MVZ 241340	GU128459	GU128495	JX838975	JX839237	JX839155	JX839061
<i>Agama sankaranica</i>	MVZ 249656	GU128460	GU128496	JX838976	–	JX839156	JX839062
<i>Agama sankaranica</i>	ZFMK 84992	GU133327	JX857586	–	–	–	–
<i>Agama spinosa</i>	JN665065	JN665065	–	–	–	–	–
<i>Agama spinosa</i>	JN665066	JN665066	–	–	–	–	–
<i>Agama spinosa</i>	MVZ 236458	GU128461	GU128497	JX838977	JX839238	JX839157	–
<i>Agama spinosa</i>	MVZ 236459	JX668211	JX857565	JX838978	JX839239	JX839158	JX839063
<i>Agama spinosa</i>	MVZ 241334	JX668212	JX857618	JX838979	JX839240	JX839159	JX839064
<i>Agama spinosa</i>	MVZ 241335	JX668213	JX857545	JX838980	JX839241	JX839160	JX839065
<i>Agama tassiliensis</i>	JN665061	JN665061	–	–	–	–	–
<i>Agama tassiliensis</i>	JN665062	JN665062	–	–	–	–	–
<i>Agama tassiliensis</i>	JN665063	JN665063	–	–	–	–	–
<i>Agama tassiliensis</i>	JN665064	JN665064	–	–	–	–	–
<i>Agama turuensis</i>	ZFMK 74930	JX668214	–	–	–	–	–
<i>Agama weidholzi</i>	AMNH 109810	JX668215	JX857591	JX838981	JX839242	JX839161	JX839066
<i>Agama weidholzi</i>	TR 481	GU128462	GU128498	JX838982	JX839243	JX839162	JX839067
<i>Agama weidholzi</i>	TR 482	JX668216	JX857554	JX838983	JX839244	JX839163	JX839068
<i>Agama weidholzi</i>	ZFMK 75001	GU133328	JX857564	JX838984	JX839245	JX839164	–
<i>Calotes versicolor</i>	MVZ 248401	JX668217	JX857560	JX838985	JX839246	JX839165	JX839069
<i>Laudakia stellio</i>	MVZ 230213	GU128464	GU128500	JX838986	JX839247	JX839166	JX839070
<i>Phrynocephalus mystaceus</i>	MVZ 245941	JX668218	JX857553	JX838987	JX839248	JX839167	JX839071
<i>Pseudotrapelus sinaitus</i>	SBED 11271	JX668219	JX857606	JX838988	JX839249	JX839168	JX839072
<i>Trapelus agnetae</i>	ZFMK 86579	JX668220	–	–	–	–	–
<i>Trapelus boehmei</i>	MNHN II	JX668221	JX857584	JX838922	JX839250	JX839111	JX839073
<i>Trapelus boehmei</i>	ZFMK49664	HQ901112	–	–	–	–	–
<i>Trapelus mutabilis</i>	ZFMK 64395	HQ901114	GU128501	–	–	JX839170	–
<i>Xenagama batillifera</i>	ZFMK 83411	JX668222	–	–	–	–	–
<i>Xenagama batillifera</i>	ZFMK 83412	JX668223	–	–	–	–	–
<i>Xenagama batillifera</i>	ZFMK 84370	JX668224	JX857572	JX838990	–	–	–
<i>Xenagama sp. nov.</i>	AMNH 105545	JX668225	JX857585	JX838991	JX839251	JX839171	JX839074
<i>Xenagama sp. nov.</i>	AMNH 105546	JX668226	JX857576	JX838992	JX839252	JX839172	JX839075
<i>Xenagama taylori</i>	MVZ 241356	GU128466	GU128502	JX838993	JX839253	JX839173	JX839076
<i>Xenagama taylori</i>	MVZ 241361	JX668227	JX857578	JX838994	JX839254	JX839174	JX839077
<i>Xenagama taylori</i>	ZFMK 75072	JX668228	JX857568	–	–	–	–

Table 2
Primers used for PCR and Sanger sequencing.

Locus	Primer Name: Sequence (5'–3')	Citation
CMOS	F: GCGGTAAGCAGGTGAAGAAA R: TGAGCATCAAAGTCTCAAT	Saint et al. (1998)
NT3	F: ATATTCTCGCTTTTCTCTGTGGC R: GCGTTTCATAAAATATTGTTGACCGG	Noonan and Chippindale (2006)
PNN	F: ACAGGTAATCAGCACAATGAYGTAGA R: TCTYTGCTGCTGAYGACTACTYCTGA	Townsend et al. (2008)
R35	F: GACTGTGGAYGAYCTGATCAGTGTGGTCC R: GCCAAAATGAGSGAGAARCGCTTCTGAGC	Leaché (2009)
16S	F: CGCTGTTTAAACAAAACAT R: CCGGTCTGAACCTCAGATCACGT	Leaché et al. (2009)
ND4	F: CACCTATGACTACCAAAGCTCATGTAGAAGC R: CATTACTTTTACTTGGATTGACCA	Arévalo et al. (1994)

Analyses of the concatenated data used the partitions and models identified with PartitionFinder. Maximum likelihood analyses were conducted with RAxML. All ML analyses executed 100 rapid bootstrap replicates followed by a thorough ML search under the specified model. Bayesian analyses used a modified version of MrBayes v3.2.1 that includes compound Dirichlet priors for branch lengths (Rannala et al., 2012). These branch length priors reduce the strong assumptions about the tree length imposed by the default branch length priors (i.e., exponential distributions) that cause trees to grow too long (Brown et al., 2010; Marshall, 2010). We implemented a gamma prior on the tree length, with shape (α_T) and rate (β_T) parameters = 1 (using GammaDir(1,1,1,1); Zhang et al., 2012). All nucleotide substitution model parameters were unlinked across partitions and the different partitions were allowed to evolve at different rates using the “prset ratepr = variable” command. For each Bayesian analysis we ran four concurrent chains (one cold and three heated) for 10 million generations and recorded samples every 1000 generations. The first 2000 samples were discarded as burn-in, and the remaining 8000 samples were used to summarize the posterior probability distributions for parameters. Maximum likelihood bootstrap values and Bayesian posterior probability values were joined and mapped to the Bayesian tree (i.e., the 50% majority-rule consensus tree calculated from the posterior distribution of trees) using SumLabels, a phylogenetic tree label concatenation utility in the python package DendroPy (Sukumaran and Holder, 2010).

2.1.4. Species tree estimation

A time-calibrated species tree for *Agama* was estimated with the Sanger data using *BEAST v1.7.1 (Heled and Drummond, 2010). The species tree analysis contained 146 samples belonging to 57 species (including non-*Agama* outgroup species). The site models, clock models, and gene trees were unlinked across loci. The ploidy type for each locus was specified to account for the fourfold smaller effective population size of the mtDNA relative to the nuclear genes resulting from the haploid and maternal inheritance of mtDNA (Ballard and Whitlock, 2004). The nucleotide substitution models selected using jModelTest were applied; however, difficulty in estimating overly complex models prompted us to exclude the invariant sites parameter (I) from models that also included the among-site rate variation parameter (Γ). The uncorrelated lognormal relaxed clock was applied to each locus. Twenty replicate analyses were conducted with random starting seeds and chain lengths of 400 or 600 million generations with parameters sampled every 100,000 steps. Long chains were necessary for achieving high effective sample sizes (ESS) for parameters, and ESS values ≥ 200 were used as a proxy for convergence of parameters. Species trees were summarized after discarding the first 25% of trees as burn-in. The species trees obtained across replicate runs were compared for congruence by examining their topology and

posterior probability values in Are We There Yet? (AWTY; Nylander et al., 2008). The post-burn-in samples from analyses were combined and used to summarize the posterior probability distribution of parameters.

We estimated species trees under two tree priors, a Yule prior and a birth–death prior, and compared the posterior distributions using the harmonic mean likelihood in conjunction with Bayes factors and Akaike’s information criterion through Markov chain Monte Carlo simulation (AICM; Baele et al., 2012). Under the AICM, an increase in the number of parameters penalizes more complex models, and models with lower AICM values are preferred over models with higher values.

Two calibrations were used to obtain divergence dates on the species tree following the method outlined by McCormack et al. (2010): (1) the divergence between *Calotes* and *Phrynocephalus* occurred 62.5 Ma, a date obtained by a study of squamate divergence times using 11 fossil calibrations (Wiens et al., 2006). Uncertainty in this date was accommodated using a normal prior probability distribution with a mean of 62.5 Ma and a standard deviation of 3.0 Ma, which results in 5% and 95% quantiles at 57.6 Ma and 67.4 Ma, respectively. (2) The divergence between *Xenagama* and *Pseudotrapelus* occurred between 16.4 Ma and 19.6 Ma (normal distribution, mean = 18 Ma and stdev = 1.0 Ma), which encompasses the estimates obtained using pairwise sequence divergence calculations for mtDNA (Macey et al., 2006). These two calibration points are derived from previous studies and not specific fossil calibrations, which may lead to compounded inaccuracy of estimated divergence times.

2.2. Anchored phylogenomics data

2.2.1. Molecular methods

The anchored phylogenomics data include 23 agamid lizards representing all major clades of *Agama* identified in the time-calibrated species tree, as well as two outgroups (Table 1). Anchored phylogenomics (Lemmon et al., 2012) utilizes hybrid enrichment via sequence capture to enrich for a set of 512 loci that have been pre-screened for properties amenable to phylogenetic analysis (e.g., single-copy, low repetitive DNA, few indels, etc.). Indexed libraries were prepared following a protocol modified from Kircher et al. (2011). Libraries were pooled (8 per pool) and then enriched using the v.1.0 probe set for vertebrates (Lemmon et al., 2012) through the Agilent Custom SureSelect kit. Enriched libraries were sequenced via single-end 50 bp sequencing on an Illumina HiSeq 2000 at the Florida State University Biology Core Facility. Raw sequencing reads were processed using a bioinformatics workflow that de-multiplexes and removes low quality reads, merges overlapping reads, and removes PCR duplicates (Lemmon et al., 2012). Reads were mapped to each locus, and a consensus sequence was made for each individual for each locus.

2.2.2. Alignment and partitioning

Alignments were generated for each locus using MUSCLE. The appropriate nucleotide substitution model was selected for each locus using jModelTest. This search was limited to models with three substitution schemes, estimated base frequencies, and rate variation under a gamma parameter with four rate categories. The base tree was estimated using ML optimization and nearest-neighbor interchange branch swapping. Models within the 95% confidence interval based on the BIC were retained and the most parameter rich model out of this set was chosen. The proportions of variable and informative sites were compared to the estimated model of evolution to determine if there is a correlation between model complexity and site variability. The site proportion was regressed against the number of parameters in the estimated model using the linear model function (Chambers, 1992) in

R (R Development Core Team, 2011). Uncorrected pairwise sequence divergence of the concatenated anchored phylogenomic loci and the number of variable and parsimony informative sites for each locus was estimated using PAUP* v.4.0b10 (Swofford, 2003).

2.2.3. Gene tree estimation

Maximum likelihood trees for each of the anchored phylogenomics loci were estimated using the GTRGAMMA model in RAXML. We also conducted phylogenetic analysis on the concatenated phylogenomic data. We estimated a maximum likelihood phylogeny using RAXML using the GTRGAMMA model (without locus partitioning) with 1000 bootstrap replicates. We also calculated genetic distance trees for the concatenated data using UPGMA and NJ in PAUP*.

2.2.4. Species tree estimation

We used the summary statistic approaches STEAC and STAR (Liu et al., 2009) to generate species trees from the individual ML gene trees estimated for each locus. The ML gene trees were combined into a single file and analyzed using the phybase package in R to generate the STEAC and STAR trees. We used *BEAST to estimate species trees using a subset of the genes with the largest proportion of informative sites (the top 10 and top 20 loci). For the *BEAST analyses, the substitution models were based on jModelTest, and all genes were assigned an uncorrelated log-normal clock. The species trees used a Yule prior and the population size parameter was set to constant linear. The *BEAST analyses were run with four replicates for 100 million (10 genes) or 200 million (20 genes) generations. Convergence across replicate runs was assessed using Tracer and AWTY, and retained trees were summarized using the TreeAnnotator utility in BEAST (Drummond and Rambaut, 2007).

2.3. Hybrid phylogenetic–phylogenomic approach

The final combined posterior distribution of time-calibrated species trees obtained from the *BEAST analyses of the Sanger data was filtered (based on topology only) using the preferred phylogenomic tree as a backbone constraint in PAUP*. The phylogenomic tree included a 4-way polytomy to reflect uncertainty in relationships found at the base of the tree. The filtering step retained only those topologies in the posterior distribution of time-calibrated species trees that were in agreement with the backbone constraint imposed by the phylogenomic tree. A maximum clade credibility (MCC) tree was estimated from the resultant filtered posterior distribution of species trees using TreeAnnotator. The hybrid phylogenetic–phylogenomic posterior distribution and MCC tree were used in subsequent analyses of biogeography, character evolution, and diversification.

2.4. Biogeography

The dispersal-extinction-cladogenesis model of geographic range evolution was implemented using Lagrange v0.1 (Ree et al., 2005; Ree and Smith, 2008). Information on the timing of lineage divergences was incorporated using the hybrid phylogenetic–phylogenomic species tree. Seven major biogeographic areas were defined based on a recent cluster analysis of thousands of plant and animal species (Linder et al., 2012). These include (1) Northern Africa (north of the Sahel), (2) Sahel (transition zone between the Sahara and savannas), (3) Horn of Africa, (4) West Africa (west of Cameroon), (5) South Africa (south of the Zambezi and Cunene Rivers), (6) East Africa (including the Great Rift Valley), and (7) Central Africa (core of the continent). The availability of connections between areas (dispersal routes) were unconstrained.

2.5. Trait correlations and morphological evolution

Data on body size, coloration, and mating systems of *Agama* were taken from the literature (Grandison, 1968; Joger, 1979; Moody and Böhme, 1984; Branch, 1998; Wagner et al., 2008a,b; Wagner, 2010a; Geniez et al., 2011; Wagner and Bauer, 2011; Mediannikov et al., 2012), scored from museum specimens, or made from personal observations in the field (Supplemental Appendix 1). We recorded maximum male body size observed for each species, measured in SVL (to the nearest mm) for our primary body size trait. Because lizards have indeterminate growth, we used log-transformed maximum SVL data for all analyses that included body size. Color and sociality traits were coded as discrete characters with two states. Social system was scored as either (0) solitary, or (1) colonial breeding. Male territoriality states included (0) only during breeding season, and (1) territoriality all year. Female coloration (and male throat coloration) was coded as absent (0) or present (1). Finally, male breeding coloration was coded as either (0) minor/seasonal, or (1) extensive.

Correlations among pairs of morphological and sociality traits were tested using maximum likelihood and Bayesian methods in BayesTraits v1.0 (Pagel et al., 2004; Pagel and Meade, 2006). The posterior distribution of hybrid phylogenetic–phylogenomic species trees was used in all analyses. Ancestral states and models of trait evolution were estimated using BayesMultistate (Pagel et al., 2004). Four replicate analyses were conducted for one million generations each (retaining 900 samples). Tests for correlated evolution between two binary traits were conducted using maximum likelihood and Bayesian implementations of BayesDiscrete (Pagel and Meade, 2006). The independent and discrete models were compared using likelihood ratio tests for the maximum likelihood results, and Bayes factors for the Bayesian posterior distributions. Phylogenetic ANOVA (Garland et al., 1993) was performed on log-transformed body size for each of our five discrete groupings. We used phy.anova in the Geiger R package (Harmon et al., 2008) with 1000 simulations to determine a phylogenetic *p*-value.

Morphological disparity through time (Harmon et al., 2003) was examined using the delta-disparity test (Burbrink et al., 2012). We used the R function Badbrains (Burbrink et al., 2012) to produce a distribution of Δ -MDI values that quantify morphological disparity in body size across the posterior distribution of species trees. Negative Δ -MDI values indicate low within-clade disparity, distributions centered on zero are no different from the null model of Brownian motion, and positive Δ -MDI values suggest high within-clade disparity.

2.6. Diversification

To test the null hypothesis that per-lineage speciation and extinction rates have remained constant through time, we applied the γ statistic (Pybus and Harvey, 2000), which measures whether internal nodes of a phylogeny are closer to the root than would be expected under a model of constant diversification rates ($\gamma = 0$). Significant *P* values for negative values of γ are indicative of early burst diversification followed by a deceleration in lineage accumulation. Theory predicts that gene trees will produce earlier divergences compared to species trees (Pamilo and Nei, 1988), and that gene trees should therefore be biased towards strongly negative γ values (Burbrink and Pyron, 2011). We contrasted γ values calculated for the species tree and concatenated Sanger tree (which is essentially a gene tree) to determine whether the earlier branching times expected for the concatenated tree support early burst diversification.

3. Results

3.1. Sanger data

3.1.1. Data characteristics

The nucleotide substitution models selected for each data partition are provided in Table 3, and the best-fit partitioning scheme for the 17 data blocks estimated using PartitionFinder includes seven partitions (Table 4). The codon partition blocks for the mtDNA data are in different partitions, with the exception of ND4 1st positions grouping with the tRNAs. The 3rd codon positions for the four nuclear genes grouped into the same partition. The 1st and 2nd codon positions for the nuclear genes were placed into two partitions, one contained PNN, and the other contained CMOS, NT3, and R35.

3.1.2. Gene trees

The Bayesian and ML analyses of the concatenated nuclear and mtDNA data (Fig. 1) contains several notable relationships, and most of these relationships are supported by the phylogenetic analyses of the independent loci and concatenated nuclear genes (Supplemental Appendix 1). First, the genus *Acanthocercus* is paraphyletic, and contains *Pseudotrapelus sinaitus*, *Agama robecchii*, and *Xenagama*. Second, *Agama robecchii* and *Acanthocercus annectans* form a clade, a result that is restricted to phylogenetic analyses containing the mtDNA data. Third, *Acanthocercus yemenensis* is the sister taxon to the remaining members of “*Acanthocercus*.” Fourth, *Acanthocercus atricollis* is the sister taxon to the genus *Xenagama*. Fifth, the initial divergences within *Agama* are weakly supported, which renders the order of relationships of the major clades tenuous. Finally, population samples for some species within *Agama* do not form exclusive groups, including *A. agama*, *A. lionotus*, and *A. boueti*.

3.1.3. Species tree

The BEAST species tree analyses using the Yule tree prior were favored over the birth–death tree prior. The Bayes factor (2logBF) calculated from the harmonic mean of the marginal likelihoods

Table 3

Nucleotide substitution models (selected out of 24 candidate models) for the nuclear and mitochondrial gene data blocks based on the Bayesian information criterion using jModelTest.

Data blocks	Model
Nuclear genes	GTR+I+G
PNN	GTR+I+G
1st positions	GTR+G
2nd positions	GTR+G
3rd positions	K80+G
R35	GTR+I+G
1st positions	SYM+I+G
2nd positions	K80+I+G
3rd positions	HKY+G
NT3	GTR+I+G
1st positions	GTR+I+G
2nd positions	K80+I+G
3rd positions	SYM+G
CMOS	HKY+I+G
1st positions	K80+I+G
2nd positions	K80+I+G
3rd positions	GTR+I+G
Mitochondrial genes	GTR+I+G
16S	GTR+I+G
tRNA	GTR+G
ND4	GTR+I+G
1st positions	GTR+I+G
2nd positions	GTR+I+G
3rd positions	GTR+G

Table 4

Best-fit partitioning scheme for the 17 data blocks using the Bayesian information criterion in PartitionFinder.

Partition	Best Model		Data blocks in partition
	MrBayes	RAxML	
1	GTR+I+G	GTR+I+G	ND4-1st, tRNA
2	GTR+I+G	GTR+I+G	ND4-2nd
3	GTR+G	GTR+G	ND4-3rd
4	GTR+I+G	GTR+I+G	16S
5	K80+G	GTR+G	CMOS-3rd, NT3-3rd, PNN-3rd, R35-3rd
6	GTR+G	GTR+G	PNN-1st, PNN-2nd
7	SYM+I+G	GTR+I+G	CMOS-1st, CMOS-2nd, NT3-1st, NT3-2nd, R35-1st, R35-2nd

was 8.2, or 82 times more likely in favor of the Yule model versus the birth–death model. The model comparison based on Akaike's information criterion through MCMC simulation ranked the Yule model (−86,548.4) over the birth–death model (−86,611.1).

The final combined posterior distribution of time-calibrated species trees from the separate BEAST analyses contained 16,382 trees. The MCC species tree (Fig. 2) supports the same notable relationships outlined for the concatenated phylogeny. These relationships include the paraphyly of *Acanthocercus*, and the placement of *Agama robecchii* in the “*Acanthocercus*” clade. The species tree does not provide evidence for the exclusivity of *Agama agama*, *A. lionotus*, or *A. boueti*, because we assumed that these species were independent lineages prior to conducting coalescent-based species tree inference.

The time-calibrated species tree indicates that diversification within *Agama* began approximately 23 Ma (95% HPD = 18.6–27.4 Ma), a timeframe that is contingent upon the calibration priors (Fig. 2). The species tree indicates that *Agama* is partitioned into at least five regional species assemblages, including, West, East, Sahel, Southern, and Northern clades. The support for each of these clades is typically strong (posterior probability values ≥ 0.95), but the support for the interrelationships among these major groups is weak (posterior probabilities <0.95).

Achieving convergence between BEAST analyses with the multilocus data, which included missing data for some species across multiple loci, proved difficult. While most of the 20 independent chains produced similar likelihood estimates, four of the analyses did not converge on similar posterior probabilities (e.g., the likelihood and model parameters), and were trapped on local optima for up to 300 million generations. Convergence diagnostics are provided in Supplemental Appendix 1.

3.2. Anchored phylogenomics data

3.2.1. Data characteristics

The anchored phylogenomics approach provided 215 loci with complete sampling for the 21 *Agama* and two outgroup species. The loci were trimmed to maximize coverage, resulting in alignments with no missing data. The 215 loci totaled 71,614 bp with an average length of 333 bp (range 200–643 bp). We note that both the number and lengths of compete loci could be increased substantially by increasing sequencing effort (i.e., 150 bp paired-end reads instead of 50 bp single-end reads). These data contained an average of 7.5% parsimony informative (range 0–16.9%) and 14.5% variable (range 0.8–26.5%) sites within loci (Fig. 3), and uncorrected pairwise sequence divergence between species averaged 2.5% within *Agama* and 4.5% from *Agama* to the outgroup taxa. Model testing preferred models with gamma to accommodate rate variation (Fig. 4). The K80 model was selected most often, followed by the HKY model, suggesting that the genomic regions associated with these loci have equal base frequency and a transition/transversion bias (Fig. 4). A

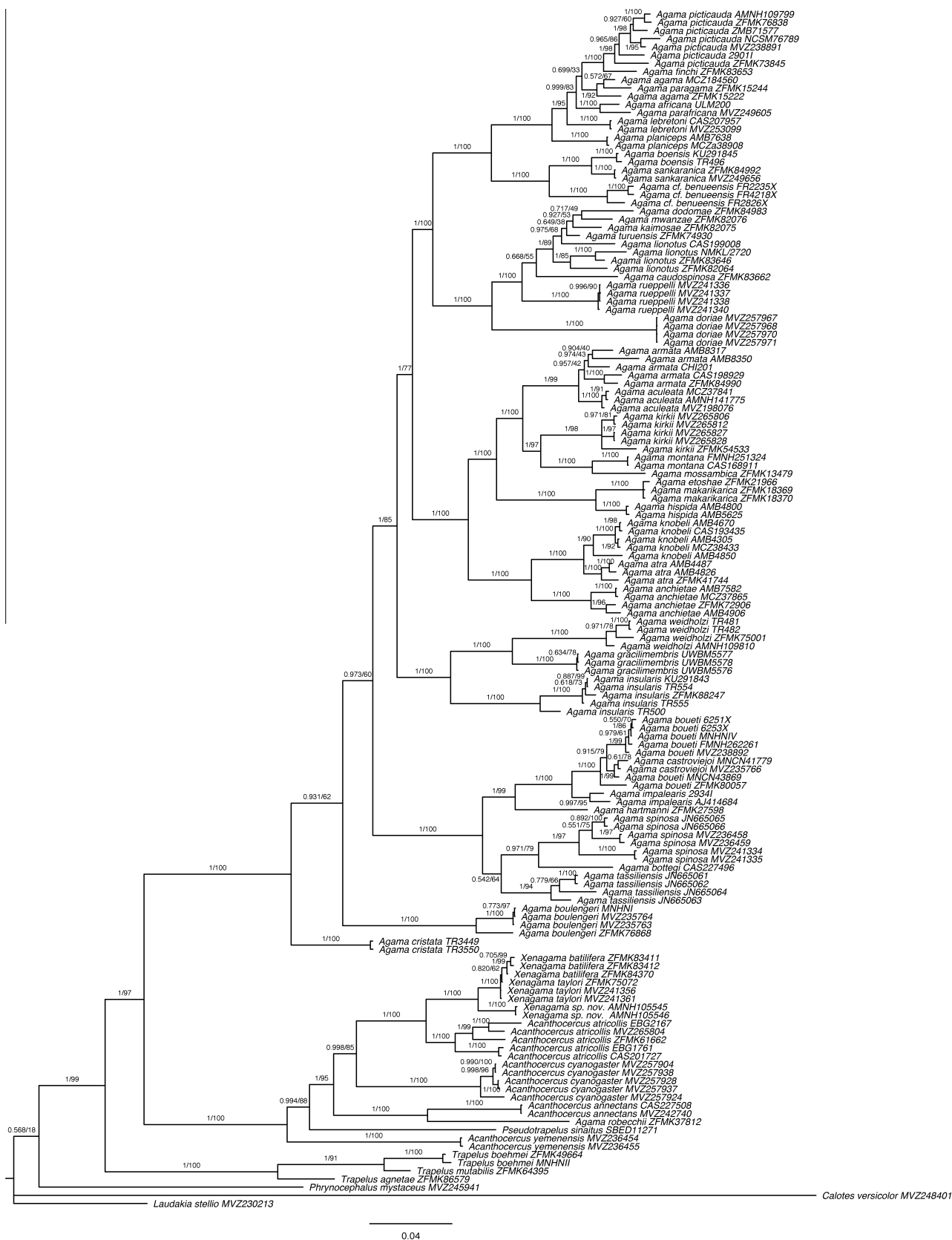


Fig. 1. Concatenated data phylogeny (mtDNA + four nuclear genes) for African *Agama* based on a Bayesian phylogenetic analysis using MrBayes. Posterior probability values ≥ 0.50 and RAxML bootstrap values $\geq 50\%$ are shown on branches.

regression of the proportion of variable and informative sites against models selected by jModelTest indicated model selection is not correlated with site variability (Fig. 4).

3.2.2. Gene trees

The concatenated ML tree of the 215 loci recovered 100 percent bootstrap support for all nodes, with the exception of the two

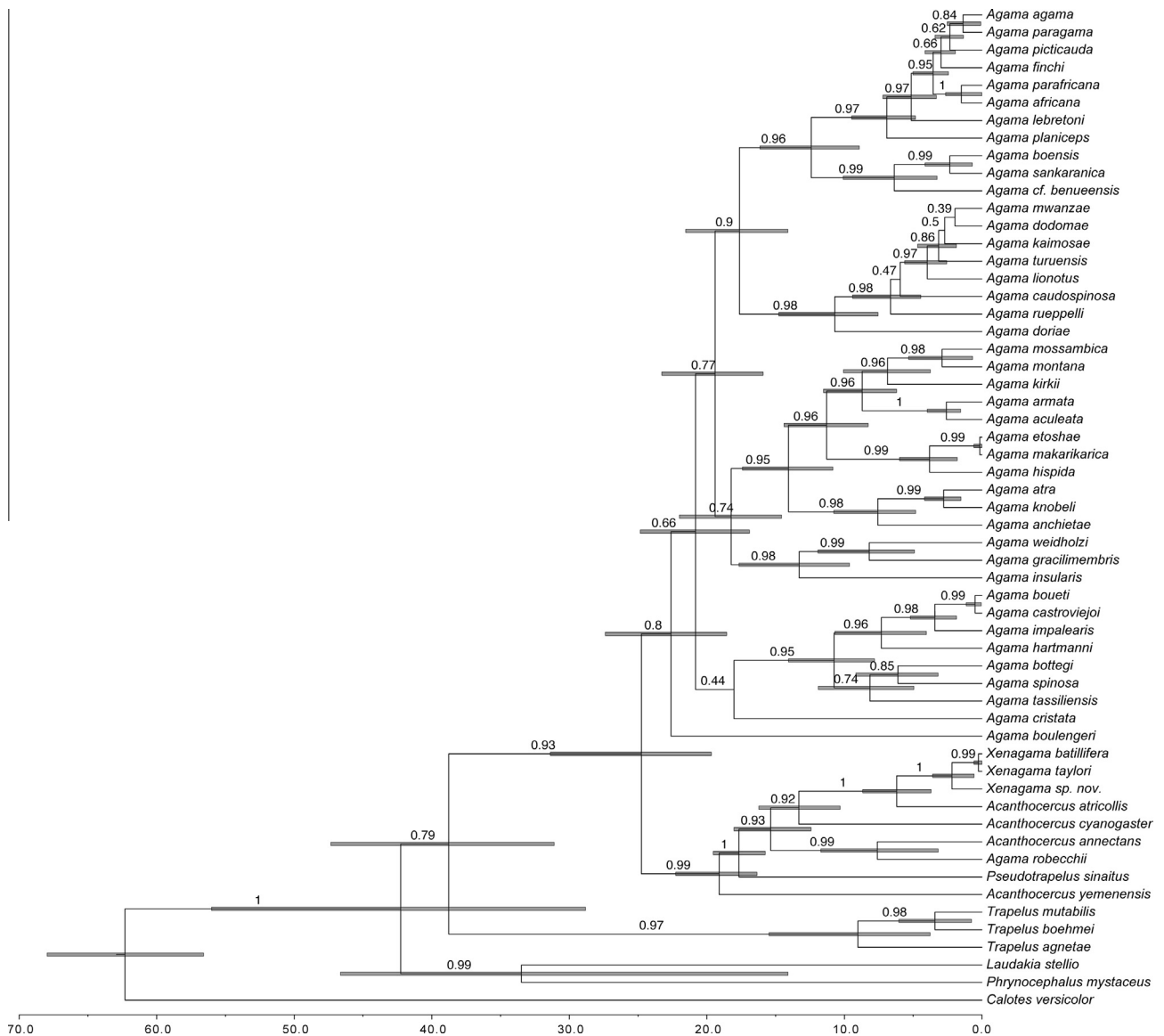


Fig. 2. Time-calibrated Bayesian species tree for African *Agama* estimated using [†]BEAST (mtDNA + four nuclear genes) for the Markov chains that reached apparent stationarity. Numbers on nodes are posterior probability values. Horizontal bars indicate the 95% HPD for divergence times (in millions of years).

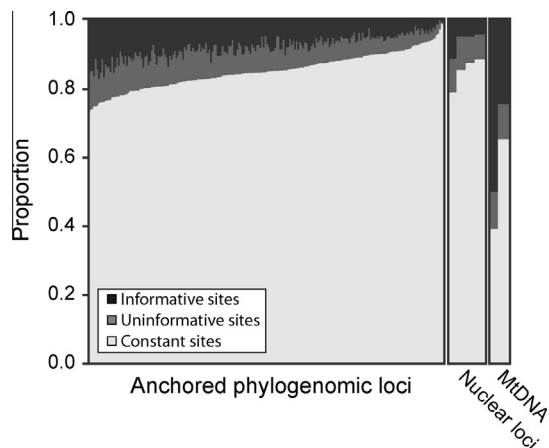


Fig. 3. Site variability in the 215 anchored phylogenomics loci, four nuclear loci, and two mitochondrial genes, ordered by proportion of informative sites.

nodes supporting the initial divergences within *Agama* (Fig. 5). These two nodes have bootstrap values of 72 and 48, and the ML topology differs from the species tree analysis of the Sanger data (Fig. 2). To explore how each of the 215 loci supported the base of the *Agama* phylogeny, we conducted ML analyses for each locus. First, we collapsed the phylogeny into a four-way polytomy at the base of *Agama*, which has 15 possible rooted solutions. Backbone constraint trees for each of these 15 possible topologies were used to determine which was supported by each of the 215 loci. For each locus, we maximized the likelihood for each of the 15 topologies in PAUP[†], using the preferred model selected from jModelTest. We enforced a molecular clock to keep the trees rooted. The ML topologies for each of the 215 loci recovered all 15 possible alternate topologies for these basal nodes, with some genes supporting multiple topologies (Table 5). Of the 15 possible solutions, the topologies placing the clade containing *Agama bottegi*, *A. boueti*, and *A. spinosa* at the base were recovered most frequently (Table 5).

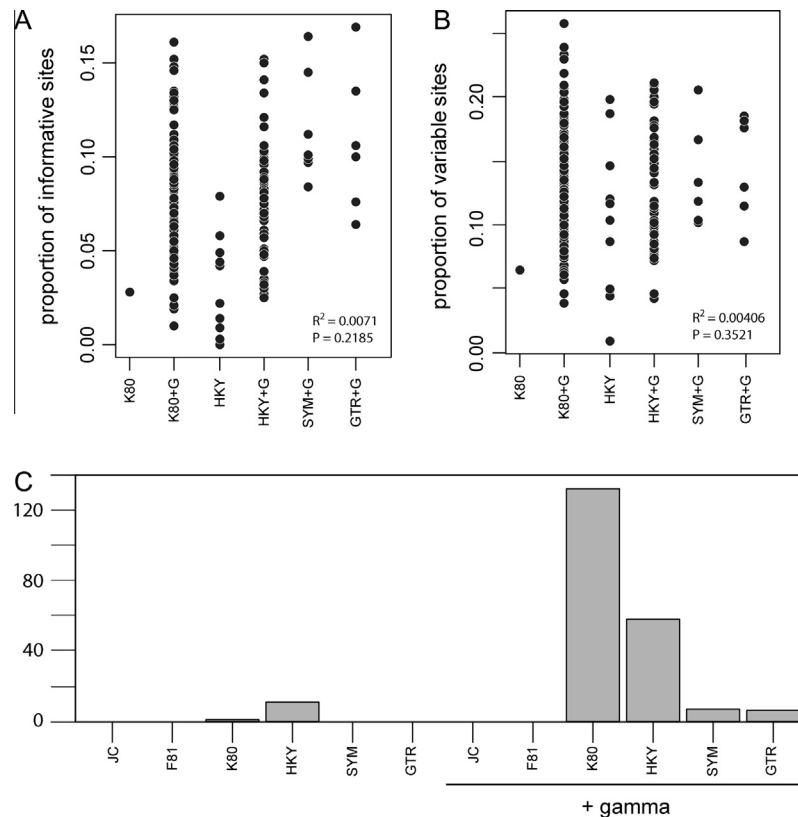


Fig. 4. The proportion of informative sites (A) and proportion of variable sites (B) for the 215 anchored phylogenomics loci, arranged by substitution model (selected using jModelTest). Twelve substitution models were evaluated, and models incorporating the gamma parameter were preferred (C).

3.2.3. Species trees

The species tree topologies estimated from the phylogenomic data differ from the ML tree estimated for the concatenated data (Fig. 5). The topological differences concern the placement of *Agama boulengeri* in relation to the two nodes with low bootstrap support in the ML tree. The ML tree places *A. boulengeri* as the sister taxon to all other *Agama*. The STAR tree places *A. boulengeri* as the sister taxon to a clade containing *A. bottegi*, *A. boueti*, *A. spinosa*, *A. gracilimembris*, *A. insularis*, and *A. weidholzi*. The STEAC and BEAST topology (the same topology as UPGMA and NJ) places the clade containing *A. bottegi*, *A. boueti*, and *A. spinosa* as sister to the rest of *Agama*, and *A. boulengeri* sister to a clade containing *A. gracilimembris*, *A. insularis*, and *A. weidholzi*. The BEAST analyses using the top 10 or 20 most informative loci recovered the same topology, but the analysis with 20 loci provided increased support (Fig. 5).

3.3. Hybrid phylogenetic–phylogenomic approach

The Sanger data did not provide strong support for the relationships among the major clades, but the support for the backbone of the phylogeny was increased after filtering the posterior distribution of species trees (16,382 trees) for those that were congruent with the backbone constraint imposed by the topology from the phylogenomic data (Fig. 6). The filtered posterior distribution of species trees retained 206 trees, and the MCC tree calculated from this reduced posterior distribution is referred to as the hybrid phylogenetic–phylogenomic species tree (Fig. 6). This MCC species tree and/or the reduced posterior distribution was used for the analyses of biogeography, character evolution, and diversification. This species tree places *A. boulengeri* sister to all other *Agama* with weak support (posterior probability = 0.67; Fig. 6). The remaining species

are divided into five major clades arranged asymmetrically (posterior probability ≥ 0.95 ; Fig. 6). At shallow levels of divergence (i.e., ≤ 5 mya), relationships are weak among species within the East African *A. lionotus* complex and the West Africa *A. agama* complex (Fig. 6), two understudied groups that may harbor additional cryptic species diversity.

3.4. Biogeography

The dispersal–extinction–cladogenesis model of geographic range evolution suggests that monophyletic radiations of *Agama* have been established in Southern, East, West, and Northern Africa for approximately 10 mya (Fig. 6). The biogeographic origin of *Agama* is confined to Northern or West Africa; a Northern origin follows intuition since the biogeographic distribution of the clade sister to *Agama* is mostly North and Northeastern African and Middle Eastern. However, the low support for the placement of the West African endemic *A. cristata* near the base of the tree introduces uncertainty into this inference. Many instances of dispersal between adjacent biogeographic regions are evident, and these movements inform the history of zoogeographic connections across Africa (Supplemental Appendix 1). For instance, the Western clade contains species distributed as far as East Africa (*A. finchi*) and southern Africa (*A. planiceps*). Thus, the once widespread Guineo-Congolian rainforest, which is now confined to fragments in West and Central Africa, retains a foothold as far to the east as the Kakamega Forest in Kenya (Wagner et al., 2008a,b). These data also implicate Angola as a biogeographic corridor that links Central and Southern Africa. In general, the Angolan lizard fauna is characterized by an extremely abrupt turnover, but with some leakage of equatorial taxa into the south (e.g., *A. planiceps*).

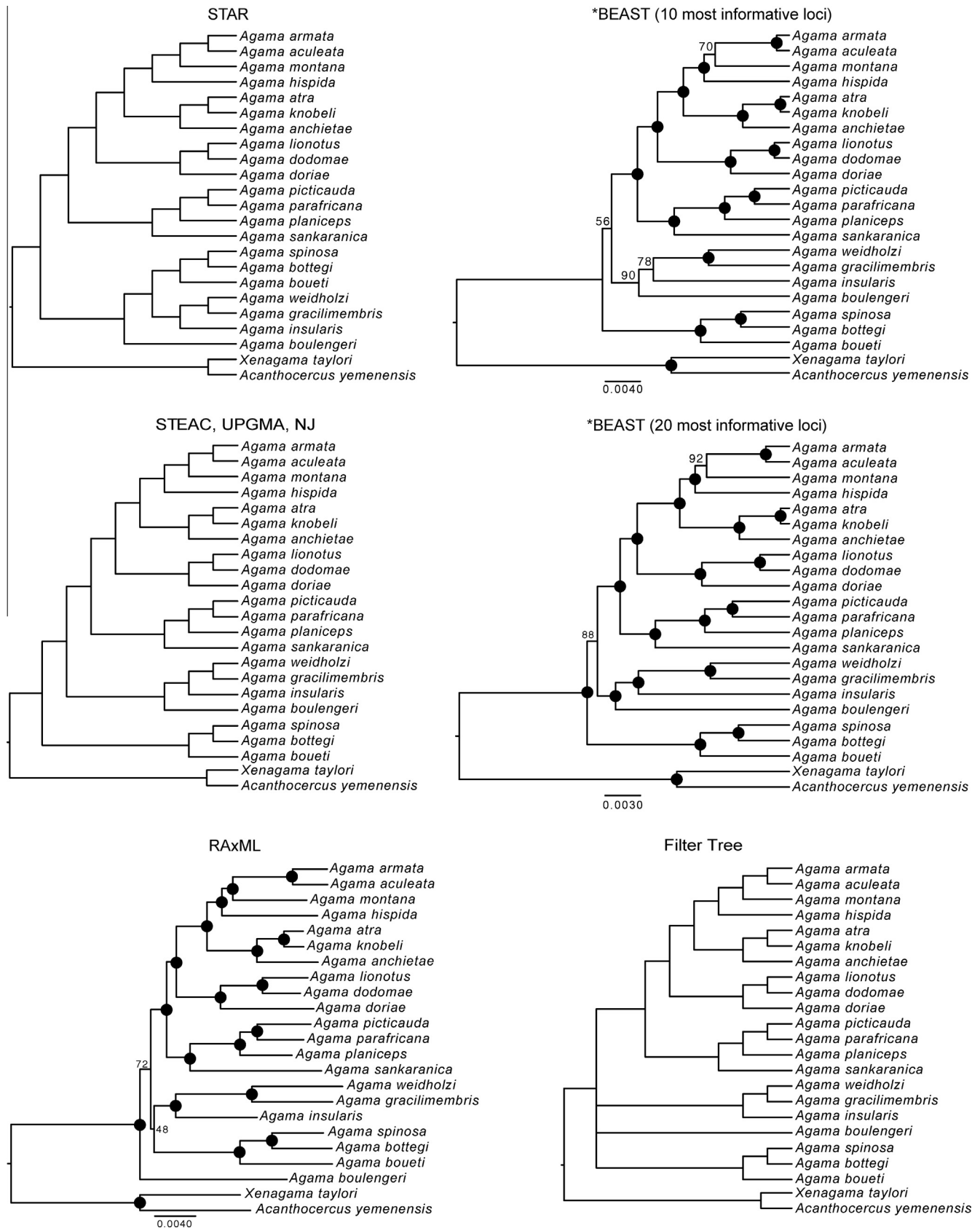


Fig. 5. Phylogenetic trees for *Agama* based on the 215 anchored phylogenomics loci. The STEAC, UPGMA, NJ, and *BEAST topologies are identical. The STAR topology differs from the others by placing the clade containing *A. spinosa*, *A. bottegi*, and *A. boueti* sister to the rest of *Agama*. The RAxML phylogeny placed *A. boulengeri* sister to remaining *Agama*. Numbers on nodes are support values (posterior probabilities or bootstrap values), and black dots indicate posterior probability values ≥ 0.95 or bootstraps = 100.

Table 5

The maximum likelihood topologies for the 215 phylogenomic loci support all 15 possible rooted topologies depicting the initial divergences within *Agama*. Some anchored phylogenomic loci supported more than one topology with the same ML score. Abbreviations in gene trees are as follows: A = *Agama boulengeri*; B = *A. bottegii*, *A. boueti*, *A. spinosa* clade; C = *A. gracilimembris*, *A. insularis*, *A. weidholzi* clade; D = remaining *Agama*.

Gene tree	Rank	Count
(B, (D, (C, A)))	1	29
(B, (C, (D, A)))	2	27
(B, (A, (D, C)))	3	26
(C, (B, (B, D)))	4	24
(A, (B, (D, C)))	5	21
(A, (C, (D, B)))	6	20
(C, (D, (B, A)))	7	17
(A, (D, (C, B)))	8	16
(D, (B, (C, B)))	9	16
(D, (C, (B, A)))	10	15
(C, (A, (D, B)))	11	14
((B, D), (C, A))	12	13
((B, A), (D, C))	13	12
(D, (B, (C, A)))	14	10
((A, D), (C, B))	15	4

3.5. Trait correlations and morphological evolution

Tests for correlated evolution in the binary traits (i.e., male breeding coloration and mating system) support the correlated evolution of these traits under maximum likelihood and Bayesian methods (Table 6). Male throat coloration and female coloration are not correlated with male breeding color using ML, but using Bayesian estimation there is a significant correlation (posterior probability = 0.99) between female coloration and male breeding color (Table 6). The instantaneous rates for forward and backward changes in traits are nearly equal for male breeding color, mating systems, and male throat color; however, rates of change in female

coloration are five times higher for gains than losses (Table 7). The posterior probabilities for trait evolution models favor the one rate (equal rate) model for male breeding color, mating systems, and male throat color (posterior probabilities ≥ 0.8), but for female coloration the equal rate model has a low posterior probability = 0.43 (Table 7). The phylogenetic ANOVA supports correlations between male body size and male breeding color, mating system, and male territoriality ($P < 0.0001$), but body size correlations with female color or male throat pattern are non-significant ($P > 0.5$).

Within each biogeographic region, we see the repeated association among a suite of sexually dimorphic traits (Fig. 7). Specifically, large males typically have colorful secondary sexual characteristics, whereas small males are drab and tend to lack extensive coloration.

Relative morphological disparity through time in *Agama* is higher than that predicted under a Brownian motion model (Fig. 8). This indicates that most variation is found within clades with a burst of morphological disparity starting approximately 20 mya coinciding with the diversification of *Agama* into different biogeographic regions of Africa. High within-clade morphological diversification is also indicated by a positive Δ-MDI distribution (Fig. 8).

3.6. Diversification

A constant rate diversification model cannot be rejected for *Agama* using the γ statistic, which supports a steady increase in lineage accumulation through time (Table 8). This result is robust when using the MCC species tree ($\gamma = -1.013$, $P = 0.155$; Table 8). However, the Sanger concatenation tree rejects the constant rate diversification model in favor of an early burst model with a slowdown in lineage accumulation through time ($\gamma = -1.754$; $P = 0.039$; Table 8). A large portion of the posterior distribution for the concatenated

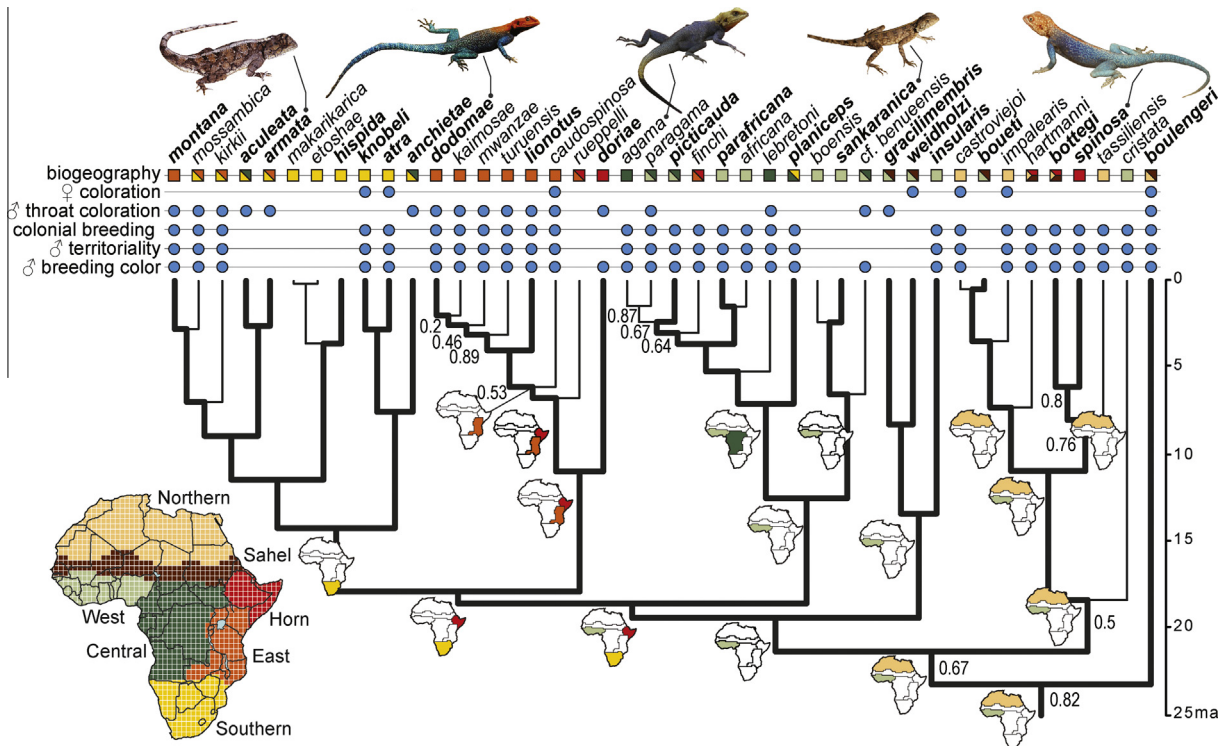


Fig. 6. Hybrid phylogenetics–phylogenomic species tree for African *Agama*, and biogeographic relationships across the continent. The Sanger data (mtDNA and four nuclear genes) were used to estimate a time-calibrated species tree using BEAST (Fig. 2). This posterior distribution of species trees was then filtered using the anchored phylogenomics tree (215 loci; Fig. 5 “Filter Tree”) as a backbone constraint. The branches connecting the 23 species with anchored phylogenomics data are highlighted in bold. Bayesian posterior probabilities for clades ≥ 0.95 are not shown.

Table 6

Trait correlations with male breeding color in *Agama* lizards tested with maximum likelihood and Bayesian methods in BayesTraits. Correlations with male breeding color indicated in bold exceed standard statistical significance levels.

Male breeding color	Maximum likelihood ^a			Bayesian estimation ^c		
	Dependent model ^b	Independent model ^c	LRT ^d	Dependent model	Independent model	BF ^f
+♂ throat coloration	−42.39	−43.78	2.77	0.92	0.08	5.9
+♀ coloration	−34.37	−39.07	9.41	0.99	0.01	1.8
+mating system	−26.85	−43.53	33.36	1.0	0.0	39.5

^a Marginal log likelihood averaged across 10 runs.

^b Number of model parameters = 8.

^c Number of model parameters = 4.

^d Likelihood ratio test.

^e Averaged over the posterior distribution of trees.

^f Bayes factor.

Table 7

Bayesian estimation of trait evolution in *Agama*. Estimated values are averages over the posterior probability distribution of the hybrid phylogenetic–phylogenomic species tree.

Trait	ln(L) ^a	q_{01} ^b	q_{10} ^c	Pr(model) ^d				
				Z0	10	00	01	OZ
Male breeding coloration 0 = minor/seasonal 1 = extensive	−25.48	0.24	0.22	0.14	0.01	0.82	0.00	0.03
Mating system ^e 0 = solitary male 1 = colony	−26.04	0.72	0.71	0.17	0.00	0.80	0.00	0.02
Female coloration 0 = absent 1 = present	−22.72	0.36	1.54	0.18	0.14	0.43	0.18	0.07
Male throat color 0 = absent 1 = present	−26.33	0.86	0.86	0.00	0.00	0.94	0.00	0.06

^a Marginal log likelihood.

^b The mean of the instantaneous rate of forward change integrated over all models.

^c The mean of the instantaneous rate of backward change integrated over all models.

^d Posterior probability for trait evolution models: Z0 (1 rate, $q_{ij} > 0$, $q_{ji} = 0$); 00 (1 rate, $q_{ij} = q_{ji}$); OZ (1 rate, $q_{ij} = 0$, $q_{ji} > 0$); 10 (2 rates, $q_{ij} > q_{ji}$); 01 (2 rates, $q_{ij} < q_{ji}$).

^e Mating system and male territoriality are linked in *Agama*.

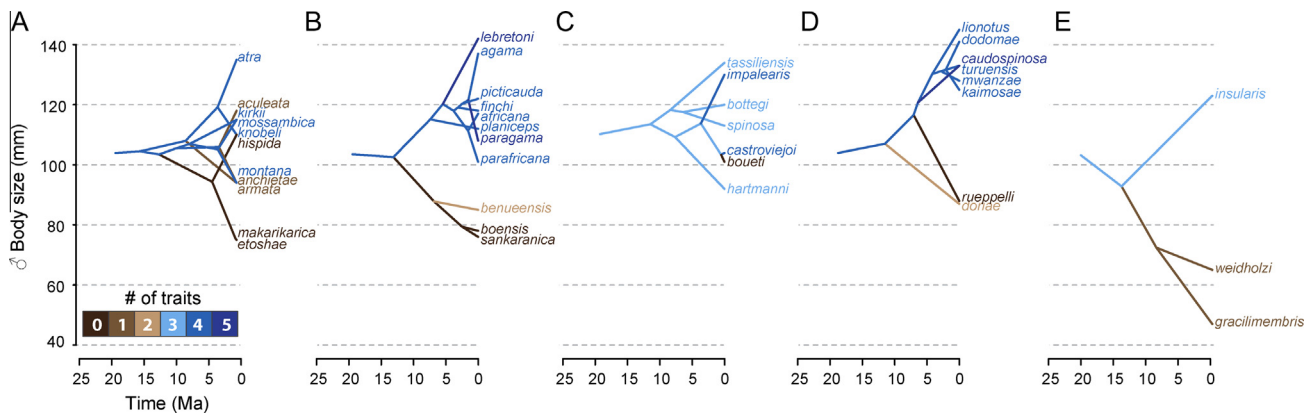


Fig. 7. Phenograms of *Agama* male body size show high levels of morphological disparity within clades occupying different biogeographic regions of Africa: (A) Southern clade, (B) West clade, (C) Northern clade, (D) East clade, (E) West/Sahel Clade. The repeated evolution of sexually selected traits (branches and species are color coded by absolute number of traits) accompanies dispersal into new biogeographic areas. (For interpretation of the references to color in this figure legend, the reader is referred to the web version of this article.)

Sanger data supports significant negative γ values (66.6%; Table 8). This contrasts with the posterior distribution of species trees, in which only 1.4% support significant negative γ values.

4. Discussion

4.1. Phylogenomics

The hybrid phylogenetic–phylogenomic approach taken here accomplishes the task of combining dense taxonomic sampling for time-calibrated species tree inference, while also including

the valuable information gained from the phylogenomic data. However, the hybrid approach does have some limitations. The final tree is driven by the initial posterior distribution of trees generated by the Sanger data, and the utility of the phylogenomic data is limited to that of a filtering device. Another approach that could be taken would be to conduct species tree inference with topological constraints that enforce the phylogenomic relationships. This would allow the MCMC analysis to sample from the stationary distribution without any need for post hoc tree filtering. In our study, the estimated divergence times for the hybrid species tree are based solely on the Sanger data, and do not include the coalescent

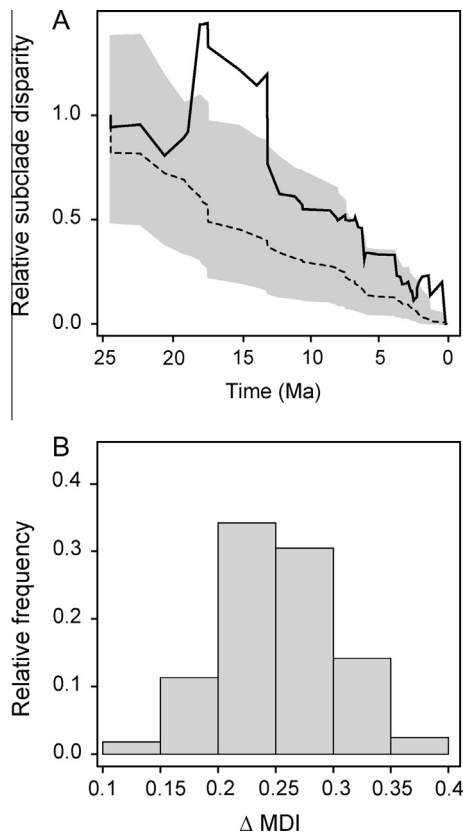


Fig. 8. (A) Relative subclade disparity through time for morphological traits in *Agama* (solid line) is higher than that predicted under a Brownian motion model (gray indicates results from 10,000 simulations; dashed line is simulation median). Most variation is found within clades with a burst of morphological disparity coinciding with diversification into different areas of Africa starting approximately 20 mya. (B) Histogram of the relative disparity through time estimates represented as Δ -MDI scores calculated over the posterior probability distribution of *Agama* species trees.

Table 8

Summary of the γ statistic for the hybrid phylogenetic–phylogenomic species tree and the concatenation tree. Results are provided for the maximum clade credibility trees (MCC) and the posterior distributions. A significant P value ($P < 0.05$) for negative γ is indicative of early burst diversification followed by a deceleration in lineage accumulation.

Tree type	γ Statistic MCC tree	P value	Trees with significant negative γ across the posterior distribution (%)
Species tree ^a	−1.013	0.155	1.4
Concatenation ^b	−1.754	0.039	66.6

^a Hybrid phylogenetic–phylogenomic species tree (Fig. 6).

^b Concatenated phylogeny from the Sanger sequence data (Fig. 1).

time information from the 215 phylogenomic loci. The addition of 215 loci improved the support among the major clades of *Agama*, but these data did not resolve the topological conflict near the base of the *Agama* tree.

Analyzing large numbers of loci remains a challenge in phylogenetics. Coalescent-based summary statistic approaches such as STEAC and STAR (Liu et al., 2009) offer alternative strategies for estimating species trees from phylogenomic data that do not have the computational limitations of BEAST. However, the summary statistic approaches are tenable at the sacrifice of information content (they use the gene trees as primary data), and therefore they typically require more data to obtain accurate results (Liu et al., 2009). Newer implementations of these methods use bootstrapping of gene trees to provide measures of clade support for the

species tree, which might make it easier to contrast different summaries of the data. Other potential solutions for injecting support measures into these summary statistic approaches include analyzing random subsets of loci and quantifying support for branches across a set of results (Liu et al., 2009), or running the methods many times while sampling gene trees from their posterior distributions (Faircloth et al., 2012).

4.2. Systematics of African agamid lizards

The number of molecular systematic investigations of *Agama* lizards has grown in recent years, and most studies have focused on specific geographic regions instead of monophyletic groups (Geniez et al., 2011; Gonçalves et al., 2012; Mediannikov et al., 2012). Our emphasis on continental-wide diversification patterns enables us to estimate the relationships among almost all described *Agama* species and therefore identify natural groupings, which are not necessarily constrained to geographic regions. We find moderate support for the monophyly of *Agama* with respect to a sister clade of African genera that includes *Acanthocercus*, *Pseudotrapelus*, and *Xenagama*. *Agama robecchii* is included in the sister clade of *Agama* (Figs. 1 and 2), and is currently being reallocated to a different genus.

The West African species *Agama agama* has been the most challenging species to define (Wagner et al., 2009), which has previously contained more than ten subspecies. Refining the species limits within *A. agama* began with the realization that several East African populations with similar adult male coloration (e.g., blue bodies with orange heads) were in fact different species (Böhme et al., 2005). We now recognize these big, blue-bodied, orange-headed *Agama* species from all regions of Africa as belonging to deeply divergent clades (Figs. 6 and 7). Herein, we follow the definition of *A. agama* according to (Wagner et al., 2009) and recognize *A. wagneri* (Mediannikov et al., 2012) as a synonym of *A. agama*. For many of the remaining populations found across West Africa, the name *A. picticauda* Peters, 1877 is available. The deep genetic splits separating many *Agama* species are masked when considering only morphology and coloration, and this leads to a high potential for discovering additional cryptic diversity as populations are investigated in greater detail using multilocus genetic data.

4.3. Biogeography

The geographic limits of the major biogeographic clades of *Agama* show some correspondence to the seven biogeographical regions for sub-Saharan Africa identified by a recent cluster analysis of thousands of plant and animal species (Wagner, 2010b; Linder et al., 2012). Our biogeographic analysis of *Agama* supports a close relationship between East and Southern African species (Fig. 6), and an arid corridor between these groups is expected in birds, snakes, and amphibians, but not necessarily in mammals (Linder et al., 2012). The Cunene and Zambezi Rivers are traditional boundaries separating these regions, but they do not appear to have acted as natural dispersal barriers in the genus *Agama*. For example, the Southern Africa clade contains three colorful and rupicolous or arboreal species (e.g., *A. kirkii*, *A. mossambica*, and *A. montana*) that occur north of the Zambezi River and are arguably components of the East African fauna. In addition, their placement within the Southern African clade further illustrates that morphology, coloration, and behavior are labile traits in *Agama* that can mislead morphology-based species relationships.

Today, African savannas, the predominant habitat type for *Agama* lizards, are among the most understudied biomes in the world (Kier et al., 2005; Lorenzen et al., 2012). Although *Agama* species only inhabit the margins of rainforests, their diversification is influenced by long-term historical fluctuations in the size and

location of this biome. A major decline in rainforest cover about 10 mya (Kissling et al., 2012), corresponding to a time of savanna expansion, coincides with the time when radiations of *Agama* were diversifying throughout most geographic areas of Africa. Among these regional clades of *Agama*, those with the highest diversification occur in topographic heterogeneous areas, such as Southern, West, and East Africa. The relatively young species complexes in East Africa (e.g., the *A. lionotus* complex) and West Africa (e.g., the *A. agama* complex) contain many species that are restricted to small geographic areas. This pattern contrasts with that found in the Sahel corridor and Africa north of the Sahara where we find some of the most geographically widespread species that are relatively older. Southern Africa is a region of diversification and glacial refuge for other arid adapted reptiles (Barlow et al., 2013; Bauer and Lamb, 2005; Stanley et al., 2011). Two ecologically similar and range-restricted species in Southern Africa, *A. etoshae* and *A. makarikarica*, are associated with geologically young habitats bordering the Etosha and Makgadikgadi pans, respectively, which were separated by the Kalahari dune system in the Pleistocene (Heine, 1989).

4.4. Diversification and character evolution

Diversification within *Agama* began approximately 23 Ma, and separate radiations in Southern, East, West, and Northern Africa have been diversifying for >10 Myr. The repeated evolution of a suite of sexually selected traits has resulted in regional *Agama* assemblages comprised of (a) sexually dimorphic species with large, colorful males that control harems of drab females, and (b) sexually monomorphic species with small, drab or only seasonally colorful males that are not easily distinguishable from females and are solitary for most of the year. The repeated evolution of these traits creates a signal of high morphological variation within clades.

Species diversification analyses using molecular phylogenies typically report patterns of early bursts of diversification (Burbrink et al., 2012; Reddy et al., 2012; Schenk et al., 2013). Our study provides new empirical evidence demonstrating that species trees and gene trees support different diversification patterns. An early burst pattern of diversification is not supported for *Agama* when using a species tree, but using gene concatenation yields the common pattern of early burst diversification (Table 8). Therefore, the method of inference used to estimate divergence times (i.e., gene tree versus species tree) may account for the diversification patterns reported in some studies. It is possible that the common reporting of early burst speciation is a methodological artifact that could be avoided by using species trees, or that constant processes of diversification, while important, are simply underreported (Moen and Morlon, 2014).

Data archival locations

Dryad DOI information (<http://dx.doi.org/10.5061/dryad.4kt16>) will be available for the following data files after acceptance:

- Anchored phylogenomic data (nexus format).
- Sanger data alignment, concatenated (nexus format).

NCBI Genbank: Nucleotide sequences for new Sanger sequences include Accession Nos. JX668128–JX668228, JX838886–JX839254, JX857543–JX857633.

Acknowledgements

This research was funded in part by a National Science Foundation grant awarded to A.D.L. (DEB-1144630). We thank

J. Felsenstein, L. Harmon, R. Harris, and J. Oaks for comments on earlier versions of the manuscript. We thank J. Sukumaran for adding the SumLabels program into the DendroPy package, and for his helpful advice on implementing alignments with SATé. We also thank C. Zhang for incorporating compound Dirichlet priors into MrBayes 3.2.1. For tissue loans we thank S. Birks (Burke Museum of Natural History and Culture), J. McGuire and C. Spencer (Museum of Vertebrate Zoology), D. Blackburn and J. Vindum (California Academy of Sciences), R. Brown (University of Kansas), A. Resetar (Field Museum of Natural History), and the Ambrose Monell Cryo Collection at the American Museum of Natural History. This manuscript benefited greatly from comments provided by anonymous reviewers.

Appendix A. Supplementary material

Supplementary data associated with this article can be found, in the online version, at <http://dx.doi.org/10.1016/j.ympev.2014.06.013>.

References

- Arévalo, E., Davis, S.K., Sites Jr., J.W., 1994. Mitochondrial DNA sequence divergence and phylogenetic relationships among eight chromosome races of the *Sceloporus grammicus* complex (Phrynosomatidae) in central Mexico. *Syst. Biol.* 43, 387–418.
- Baele, G., Lemey, P., Bedford, T., Rambaut, A., Suchard, M.A., Alekseyenko, A.V., 2012. Improving the accuracy of demographic and molecular clock model comparison while accommodating phylogenetic uncertainty. *Mol. Biol. Evol.* 29, 2157–2167.
- Ballard, J.W.O., Whitlock, M.C., 2004. The incomplete natural history of mitochondria. *Mol. Ecol.* 13, 729–744.
- Barlow, A., Baker, K., Hendry, C.R., Peppin, L., Phelps, T., Tolley, K.A., Wüster, C.E., Wüster, W., 2013. Phylogeography of the widespread African puff adder (*Bitis arietans*) reveals multiple Pleistocene refugia in southern Africa. *Mol. Ecol.* 22, 1134–1157.
- Bauer, A.M., Lamb, T., 2005. Phylogenetic relationships of southern African geckos in the *Pachydactylus* group (Squamata: Gekkonidae). *Afr. J. Herpetol.* 54, 105–129.
- Böhme, W., Wagner, P., Malonza, P., Lötters, S., Köhler, J., 2005. A new species of the *Agama agama* group (Squamata: Agamidae) from western Kenya, East Africa, with comments on *Agama lionotus* Boulenger, 1896. *Russ. J. Herpetol.* 12, 143–150.
- Branch, B., 1998. Field Guide to Snakes and Other Reptiles of South Africa. Ralph Curtis Books, Sanibel Island, FL.
- Brown, J.M., Hedtke, S.M., Lemmon, A.R., Lemmon, E.M., 2010. When trees grow too long: investigating the causes of highly inaccurate Bayesian branch-length estimates. *Syst. Biol.* 59, 145–161.
- Burbrink, F.T., Pyron, R.A., 2011. The impact of gene-tree/species-tree discordance on diversification-rate estimation. *Evolution* 65, 1851–1861.
- Burbrink, F.T., Chen, X., Myers, E.A., Brandley, M.C., Pyron, R.A., 2012. Evidence for determinism in species diversification and contingency in phenotypic evolution during adaptive radiation. *Proc. R. Soc. B* 279, 4817–4826.
- Chambers, J.M., 1992. Linear models. In: Chambers, J.M., Hastie, T.J. (Eds.), *Statistical Models in S*. Wadsworth, Pacific Grove, CA, pp. 95–144.
- Crawford, N.G., Faircloth, B.C., McCormack, J.E., Brumfield, R.T., Winker, K., Glenn, T.C., 2012. More than 1000 ultraconserved elements provide evidence that turtles are the sister group of archosaurs. *Biol. Lett.* 8, 783–786.
- Drummond, A.J., Rambaut, A., 2007. BEAST: Bayesian evolutionary analysis by sampling trees. *BMC Evol. Biol.* 2007 (7), 214.
- Edgar, R.C., 2004a. MUSCLE: a multiple sequence alignment method with reduced time and space complexity. *BMC Bioinformatics* 5, 113.
- Edgar, R.C., 2004b. MUSCLE: a multiple sequence alignment with high accuracy and high throughput. *Nucleic Acids Res.* 32, 1792–1797.
- Faircloth, B.C., McCormack, J.E., Crawford, N.G., Harvey, M.G., Brumfield, R.T., Glenn, T.C., 2012. Ultraconserved elements anchor thousands of genetic markers spanning multiple evolutionary timescales. *Syst. Biol.* 61, 717–726.
- Garland Jr., T., Dickerman, A.W., Janis, C.M., Jones, J.A., 1993. Phylogenetic analysis of covariance by computer simulation. *Syst. Biol.* 42, 265–292.
- Geniez, P., Padial, J.M., Crochet, P.-A., 2011. Systematics of north African *Agama* (Reptilia: Agamidae): a new species from the central Saharan mountains. *Zootaxa* 3098, 26–46.
- Gnirke, A., Melnikov, A., Maguire, J., Rogov, P., LeProust, E.M., et al., 2009. Solution hybrid selection with ultra-long oligonucleotides for massively parallel targeted sequencing. *Nat. Biotechnol.* 27, 182–189.
- Gonçalves, D.V., Brito, J.C., Crochet, P.-A., Geniez, P., Padial, J.M., Harris, D.J., 2012. Phylogeny of North African *Agama* lizards (Reptilia: Agamidae) and the role of the Sahara desert in vertebrate speciation. *Mol. Phylogenet. Evol.* 64, 582–591.
- Grandison, A.G.C., 1968. Nigerian lizards of the genus *Agama* (Sauria: Agamidae). *Bull. Br. Mus. Nat. Hist. Zool.* 17, 67–90.

- Harmon, L.J., Schulte II, J.A., Larson, A., Losos, J.B., 2003. Tempo and mode of evolutionary radiation in iguanian lizards. *Science* 301, 961–964.
- Harmon, L.J., Weir, J.T., Brock, C.D., Glor, R.E., Challenger, W., 2008. GEIGER: investigating evolutionary radiations. *Bioinformatics* 24 (1), 129–131.
- Heine, K., 1989. Some observations concerning the age of the dunes in the western Kalahari and palaeoclimatic implications. *Palaeoecol. Afr.* 21, 161–178.
- Heled, J., Drummond, A.J., 2010. Bayesian inference of species trees from multilocus data. *Mol. Biol. Evol.* 27, 570–580.
- Joger, U., 1979. Zur Ökologie und Verbreitung wenig bekannter Agamen Westafrikas (Reptilia: Sauria: Agamidae). *Salamandra* 15, 31–52.
- Kier, G., Mutke, J., Dinerstein, E., Ricketts, T.H., Küper, W., Kreft, H., Barhlott, W., 2005. Global patterns of plant diversity and floristic knowledge. *J. Biogeogr.* 32, 1107–1116.
- Kircher, M., Sawyer, S., Meyer, M., 2011. Double indexing overcomes inaccuracies in multiplex sequencing on the Illumina platform. *Nucleic Acids Res.* 2011, 1–8.
- Kissling, W.D., Eiserhardt, W.L., Baker, W.J., Borchsenius, F., Couvreur, T.L.P., Balslev, H., Svenning, J.-C., 2012. Cenzoic imprints on the phylogenetic structure of palm species assemblages worldwide. *Proc. Natl. Acad. Sci. USA* 109, 7379–7384.
- Lanfear, R., Calcott, B., Ho, S.Y.W., Guindon, S., 2012. PartitionFinder: combined selection of partitioning schemes and substitution models for phylogenetic analysis. *Mol. Biol. Evol.* 29, 1695–1701.
- Leaché, A.D., 2009. Species tree discordance traces to phylogeographic clade boundaries in North American fence lizards (*Sceloporus*). *Syst. Biol.* 58, 547–559.
- Leaché, A.D., Chong, R.A., Papenfuss, T.J., Wagner, P., Böhme, W., Schmitz, A., Rödel, M.-O., LeBreton, M., Ineich, I., Chirio, L., Bauer, A., Eniang, E.A., Baha El Din, S., 2009. Phylogeny of the genus *Agama* based on mitochondrial DNA sequence data. *Bonn. zool. Beitr.* 56, 273–278.
- Lemmon, E.M., Lemmon, A.R., 2013. High-throughput genomic data in systematics and phylogenetics. *Annu. Rev. Ecol. Evol. Syst.* 44, 99–121.
- Lemmon, A.R., Emme, S., Lemmon, E.M., 2012. Anchored hybrid enrichment for massively high-throughput phylogenomics. *Syst. Biol.* 61, 727–744.
- Li, C., Hofreiter, M., Straube, N., Corrigan, S., Naylor, G.J.P., 2013. Capturing protein-coding genes across highly divergent species. *Biotechniques* 54, 321–326.
- Linder, H.P., de Klerk, H.M., Born, J., Burgess, N.D., Fjeldsø, J., Rahbek, C., 2012. The partitioning of Africa: statistically defined biogeographical regions in sub-Saharan Africa. *J. Biogeogr.* 39, 1189–1205.
- Liu, K., Raghavan, S., Nelesen, S., Linder, C.R., Warnow, T., 2009. Rapid and accurate large-scale coestimation of sequence alignments and phylogenetic trees. *Science* 324, 1561–1564.
- Liu, L., Yu, L., Kubatko, L., Pearl, D.K., Edwards, S.V., 2009. Coalescent methods for estimating phylogenetic trees. *Mol. Phylog. Evol.* 53, 320–328.
- Liu, K., Warnow, T.J., Holder, M.T., Nelesen, S.M., Yu, J., Stamatakis, A.P., Linder, C.R., 2011. SATé-II: very fast and accurate simultaneous estimation of multiple sequence alignments and phylogenetic trees. *Syst. Biol.* 61, 90–106.
- Lorenzen, E.D., Heller, H., Siegmund, H.R., 2012. Comparative phylogeography of African savannah ungulates. *Mol. Ecol.* 21, 3656–3670.
- Macey, J.R., Schulte II, J.A., Larson, A., Ananjeva, N.B., Wang, Y., Pethiyagoda, R., Rastegar-Pouyani, N., Papenfuss, T.J., 2000. Evaluating trans-Tethys migration: an example using acrodont lizard phylogenetics. *Syst. Biol.* 49, 233–256.
- Macey, J.R., Schulte II, J.A., Fong, J.J., Das, I., Papenfuss, T.J., 2006. The complete mitochondrial genome of an agamid lizard from the Afro-Asian subfamily agaminae and the phylogenetic position of Bufoniceps and Xenagama. *Mol. Phylogenet. Evol.* 39, 881–886.
- Marshall, D.C., 2010. Cryptic failure of partitioned Bayesian phylogenetic analyses: lost in the land of long trees. *Syst. Biol.* 59, 108–117.
- McCormack, J.E., Heled, D., Delaney, K.S., Peterson, A.T., Knowles, L.L., 2010. Calibrating divergence times on species trees versus gene trees: implications for speciation history of *Aphelocoma* jays. *Evolution* 65, 184–202.
- McCormack, J.E., Hird, S.M., Zellmer, A.J., Carstens, B.C., Brumfield, R.T., 2013. Applications of next-generation sequencing to biogeography and phylogenetics. *Mol. Phylogenet. Evol.* 66, 526–538.
- Mediannikov, O., Trape, S., Trape, J.-F., 2012. A molecular study of the genus *Agama* (Squamata: Agamidae) in West Africa, with description of two new species and a review of the taxonomy, geographic distribution, and ecology of currently recognized species. *Russ. J. Herpetol.* 19, 115–142.
- Moen, D., Morlon, H., 2014. Why does diversification slow down? *Trends Ecol. Evol.* 29, 190–197.
- Moody, S.M., Böhme, W., 1984. Merkmalsvariation und taxonomische Stellung von *Agama doriae* Boulenger, 1885 und *Agama benueensis* Monard, 1951 (Reptilia: Agamidae) aus dem Sudangürtel Afrikas. *Bonn. zool. Beitr.* 35, 107–128.
- Noonan, B.P., Chippindale, P.T., 2006. Dispersal and vicariance: the complex evolutionary history of boid snakes. *Mol. Phylog. Evol.* 40, 347–358.
- Nylander, J.A.A., Wilgenbusch, J.C., Warren, D.L., Swofford, D.L., 2008. AWTY (are we there yet?): a system for graphical exploration of MCMC convergence in Bayesian phylogenetics. *Bioinformatics* 24, 581–583.
- Pagel, M., Meade, A., 2006. Bayesian analysis of correlated evolution of discrete characters by reversible-jump Markov chain Monte Carlo. *Am. Nat.* 167, 808–825.
- Pagel, M., Meade, A., Barker, D., 2004. Bayesian estimation of ancestral character states on phylogenies. *Syst. Biol.* 53, 673–684.
- Pamilo, P., Nei, M., 1988. Relationships between gene trees and species trees. *Mol. Biol. Evol.* 5, 568–583.
- Posada, D., 2008. JModelTest: phylogenetic model averaging. *Mol. Biol. Evol.* 25, 1253–1256.
- Pybus, O.G., Harvey, P.H., 2000. Testing macro-evolutionary models using incomplete molecular phylogenies. *Proc. R. Soc. Lond. B Biol. Sci.* 267, 2267–2272.
- R Development Core Team, 2011. R: A Language and Environment for Statistical Computing. R Foundation for Statistical Computing, Vienna, Austria. <<http://www.R-project.org/>>.
- Rannala, B., Zhu, T., Yang, Z., 2012. Tail paradox, partial identifiability, and the influential priors in Bayesian branch length inference. *Mol. Biol. Evol.* 29, 325–335.
- Reddy, S., Driskell, A., Rabosky, D.L., Hackett, S.J., Schulenberg, T.S., 2012. Diversification and the adaptive radiation of the vangas of Madagascar. *Proc. R. Soc. B* 279, 2062–2071.
- Ree, R.H., Smith, S.A., 2008. Maximum likelihood inference of geographic range evolution by dispersal, local extinction, and cladogenesis. *Syst. Biol.* 57, 4–14.
- Ree, R.H., Moore, B.R., Webb, C.O., Donoghue, M.J., 2005. A likelihood framework for inferring the evolution of geographic range on phylogenetic trees. *Evolution* 59, 2299–2311.
- Ronquist, F., Teslenko, M., van der Mark, P., Ayres, D.L., Darling, A., Höhna, S., Larget, B., Liu, L., Suchard, M.A., Huelsenbeck, J.P., 2012. MrBayes 3.2: efficient Bayesian phylogenetic inference and model choice across a large model space. *Syst. Biol.* 61, 539–542.
- Saint, K.M., Austin, C.C., Donnellan, S.C., Hutchinson, M.N., 1998. C-mos, a nuclear marker useful for squamate phylogenetic analysis. *Mol. Phylog. Evol.* 10, 259–263.
- Schenk, J.J., Rowe, K.C., Steppen, S.J., 2013. Ecological opportunity and incumbency in the diversification of repeated continental colonizations by Muroid rodents. *Syst. Biol.* 62, 837–864.
- Smith, B.T., Harvey, M.G., Faircloth, B.C., Glenn, T.C., Brumfield, R.T., 2014. Target capture and massively parallel sequencing of ultraconserved elements for comparative studies at shallow evolutionary time scales. *Syst. Biol.* 63, 83–95.
- Stamatakis, A., 2006. RAxML-VI-HPC: maximum likelihood-based phylogenetic analyses with thousands of taxa and mixed models. *Bioinformatics* 22, 2688–2690.
- Stanley, E.L., Bauer, A.M., Jackman, T.R., Branch, W.R., Mouton, P.L.F., 2011. Between a rock and a hard polytomy: rapid radiation in the rupicolous girdled lizards (Squamata: Cordylidae). *Mol. Phylogenet. Evol.* 58, 53–70.
- Sukumaran, J., Holder, M.T., 2010. DendroPy: a Python library for phylogenetic computing. *Bioinformatics* 26, 1569–1571.
- Swofford, D.L., 2003. PAUP*. Phylogenetic Analysis Using Parsimony (and Other Methods). Version 4. Sinauer Associates, Sunderland, Massachusetts.
- Thompson, J., Higgins, D., Gibson, T., 1994. CLUSTAL W: improving the sensitivity of progressive multiple sequence alignment through sequence weighting, position-specific gap penalties and weight matrix choice. *Nucleic Acids Res.* 22, 4673–4680.
- Townsend, T.M., Alegre, R.E., Kelley, S.T., Wiens, J.J., Reeder, T.W., 2008. Rapid development of multiple nuclear loci for phylogenetic analysis using genomic resources: An example from squamate reptiles. *Mol. Phylog. Evol.* 47, 129–142.
- Wagner, P., 2010a. Studies on African *Agama* VIII. A new subspecies of *Agama caudospinosa* Meek, 1910 (Sauria: Agamidae). *Zootaxa* 2715, 36–44.
- Wagner, P., 2010b. Diversity and Distribution of African Reptiles. Unpublished Ph.D. Thesis, University of Bonn.
- Wagner, P., Bauer, A., 2011. A new dwarf *Agama* (Sauria: Agamidae) from Ethiopia. *Breviora*, 1–19.
- Wagner, P., Krause, P., Böhme, W., 2008a. Studies on African *Agama* III. Resurrection of *Agama agama turuensis* Loveridge, 1932 (Squamata, Agamidae) from synonymy and elevation to species rank. *Salamandra* 44, 35–42.
- Wagner, P., Köhler, J., Schmitz, A., Böhme, W., 2008b. The biogeographical assignment of a west Kenyan rain forest remnant: further evidence from analysis of its reptile fauna. *J. Biogeogr.* 35, 1349–1361.
- Wagner, P., Wilms, T.M., Bauer, A.M., Böhme, W., 2009. Studies on African *Agama* V. On the origin of *Lacerta agama* Linnaeus, 1768 (Squamata: Agamidae). *Bonn. zool. Beitr.* 56, 215–223.
- Wagner, P., Freund, W., Modry, D., Schmitz, A., Böhme, W., 2011. Studies on African *Agama* IX. New insights into *Agama finchi* Böhme et al., 2005 (Sauria: Agamidae), with the description of a new subspecies. *Bonn. zool. Beitr.* 58, 25–34.
- Wiens, J.J., Brandley, M.C., Reeder, T.W., 2006. Why does a trait evolve multiple times? Repeated evolution of snakelike body form in squamate reptiles. *Evolution* 60, 123–141.
- Zhang, C., Rannala, B., Yang, Z., 2012. Robustness of compound Dirichlet priors for Bayesian inference of branch lengths. *Syst. Biol.* 61, 779–784.